

ABSTRACT

HANSON, ARIEL DAWN. Adhesion and Mechanobiology Methods to Proliferate and Osteogenically Differentiate Human Adipose-derived Adult Stem Cells. (Under the direction of Elizabeth Grace Lobo.)

Traditional methods of treating degenerative skeletal diseases and wounds are to use allografts, autografts, or artificial implants. However, these techniques are not ideal because of possible additional medical complications or limited tissue availability. The use of the patient's own mesenchymal stem cells for treatment, on the other hand, do not induce any immunogenic response and utilize cells that are in greater supply. Because of these advantages, doctors and researchers are investigating applications where mesenchymal stem cells (MSCs) can be used in tissue regeneration, often for bone restoration. Two important components to consider in tissue engineering transplants are: 1) tissue-specific cells; and, 2) a biocompatible scaffold which these cells can adhere to that provides short-term mechanical stability until the cells develop and produce an extracellular matrix in the implant site. The purpose of this research is two fold: 1) investigate a more effective method of inducing osteogenic differentiation of human adipose-derived adult stem (hADAS) cells through mechanical loading; and, 2) improve hADAS cell adhesion to a novel three-dimensional poly(L-lactic acid) scaffold using oxygen plasma treatment.

Mechanical stimulation of bone marrow-derived mesenchymal stem cells has been shown to enhance osteogenesis. However, more recent studies have shown that continuous loading of these cells results in desensitization and eventual loss of responsiveness to mechanical loading. To investigate this phenomenon in hADAS cells, cells from two donors with distinct and disparate osteogenic differentiation capabilities (i.e. high calcium deposition and low calcium deposition) were subjected to continuous loading via cyclic tensile strain,

rest insertion loading (10 seconds of rest inserted between each loading cycle), or maintained in static culture. Results revealed that rest insertion and continuous loading did not significantly alter calcium deposition in hADAS of both donors when cells were maintained in complete growth medium. However, when cells were cultured in osteogenic differentiation medium, both regimens of mechanical loading accelerated the induction of osteogenesis, as well as increased the total calcium deposition in hADAS cells of both donors compared to unstrained controls in osteogenic differentiation medium. The donor cells which innately deposited higher amounts of calcium appeared to respond more favorably to mechanical stimulation compared to the donor cells which deposited lower amounts of calcium, suggesting that perhaps cell lines that are more prone to osteogenic differentiation will respond better to mechanical stimulation compared to cell lines that are not.

The second key component of tissue engineered bone constructs are the scaffolds to which the cells adhere. Cell adherence has been linked to future proliferation and differentiation. Therefore, optimizing cell adherence to scaffolds is fundamental in perfecting a bone construct for implantation. In order to investigate the cellular adherence of hADAS cells on poly(L-lactic acid) (PLLA), hADAS cells were seeded on either oxygen plasma treated or untreated scaffolds. Over a 48 hour time period, hADAS cells were evaluated for 1) number of cells adhered to the scaffold; 2) viability; and, 3) morphology and distribution of cells throughout the three-dimensional PLLA matrix. Results from three age- and gender-matched donors showed a trend of increased number of cells adhered to oxygen plasma treated scaffolds compared to hADAS cells seeded on untreated scaffolds. In addition, morphology and distribution was accelerated in hADAS cells seeded on oxygen plasma treated scaffolds at earlier time points than those on untreated scaffolds. This enhanced early

cell spreading and distribution due to oxygen plasma treatment of scaffolds suggest that this methodology might provide a more optimal procedure of creating tissue engineered bone grafts.

Adhesion and Mechanobiology Methods to Proliferate and Osteogenically Differentiate
Human Adipose-derived Adult Stem Cells

by

Ariel Dawn Hanson

A thesis submitted to the Graduate Faculty of
North Carolina State University
in partial fulfillment of the
requirements for the Degree of
Master of Science

Biomedical Engineering

Raleigh, North Carolina

2007

APPROVED BY:

Dr. Behnam Pourdeyhimi

Dr. Albert J. Banes

Dr. Elizabeth G. Loba
Chair of Advisory Committee

DEDICATION

It doesn't matter to me what you do for a living –
I want to know
 what you ache for, and if you dare to dream
 of meeting your heart's longing

It doesn't interest me how old you are –
I want to know if you risk looking like a fool
 for love,
 for your dreams,
 for the adventure of being alive.

I want to know if you can be with your own joy
 if you can dance wildness,
And let the ecstasy fill you
 to the tips of your fingers and toes,
 without cautioning yourself
 to be careful
 to be realistic
Or to remember the limitations of being human.

I want to know if you can see beauty, even when it's not pretty
 every day
 and if you can source from your own life
 Beauty's Presence.

I want to know if you can live with your failure
 and still stand on the edge of the lake
 and shout to the silver of the full moon,
 “YES!”

It doesn't interest me where, or what, or with whom you have studied –
I want to know what sustains you from the inside
 when all else falls away.
 If you can be alone with yourself, and
 if you truly like the company you keep
 in the empty moments.

- Excerpts from “A Poem” by Oriah Mountain Woman

Liana, my inspiration.

BIOGRAPHY

Ariel Dawn Hanson was born on February 28, 1981 in Pittsburgh, Pennsylvania. She grew up in Doylestown, Pennsylvania and attended Central Bucks High School West. Following high school, Ariel entered Northeastern University to pursue a bachelor's degree in Mechanical Engineering. After graduating from Northeastern University in 2004, she left Boston to attend North Carolina State University in Raleigh, NC. Ariel completed her Masters degree in Biomedical Engineering in 2007.

ACKNOWLEDGMENTS

I'd like to thank the members of the Cell Mechanics Laboratory for their technical assistance, guidance, and friendship. I'd like to specifically thank Dr. Michelle Wall and Dr. Susan Bernacki for shaping the scientist I am today, as well as Dr. Elizabeth Lobo for continuing to believe in me.

To my friends, thank you for your support, comfort, and comic relief throughout this entire process. I would not have made it through these past three years without all of you by my side.

Finally, I would like to thank my family for being a continual source of inspiration and strength.

TABLE OF CONTENTS

LIST OF TABLES	vii
LIST OF FIGURES	viii
CHAPTER 1: INTRODUCTION AND LITERATURE REVIEW – BONE STRUCTURE, BIOMECHANICS, AND STEM CELLS	
1. BONE	1
2. STEM CELLS.....	9
CHAPTER 2: THE EFFECTS OF REST INSERTED AND CONTINUOUS CYCLIC TENSILE STRAIN ON HUMAN ADIPOSE-DERIVED ADULT STEM CELL LINES WITH DISPARATE OSTEOGENIC DIFFERENTIATION CAPABILITIES	
1. INTRODUCTION.....	22
2. MATERIALS AND METHODS	
2.1. CELL ISOLATION AND CULTURE.....	25
2.2. CHARACTERIZATION OF OSTEOGENIC DIFFERENTIATION POTENTIAL.....	26
2.3. SEEDING OF CELLS IN BIOFLEX™ CULTURE PLATES.....	26
2.4. APPLICATION OF MECHANICAL LOADING.....	27
2.5. CALCIUM DEPOSITION.....	27
2.6. CELL VIABILITY AND PROLIFERATION.....	28
3. RESULTS	
3.1. CALCIUM DEPOSITION.....	29
3.2. PROLIFERATION.....	33
4. DISCUSSION.....	34
SUMMARY.....	39
CHAPTER 3: LITERATURE REVIEW – SCAFFOLD FOR BONE TISSUE ENGINEERING	
1. GRAFTS FOR CRITICAL SIZE BONE DEFECTS.....	40
2. ARCHITECTURE OF SCAFFOLDS.....	41
3. FABRICATION TECHNIQUES.....	41

4. SCAFFOLD MATERIALS FOR TISSUE ENGINEERED BONE CONSTRUCTS.....	43
CHAPTER 4: EFFECTS OF OXYGEN PLASMA TREATMENT ON HUMAN ADIPOSE-DERIVED ADULT STEM CELL ADHERENCE TO POLY(L-LACTIC ACID) SCAFFOLDS	
1. INTRODUCTION.....	51
2. MATERIALS AND METHODS	
2.1. MANUFACTURING OF PLLA SCAFFOLDS.....	53
2.2. DETERMINATION OF PORE SIZE AND POROSITY.....	54
2.3. OXYGEN PLASMA TREATMENT OF SCAFFOLDS.....	56
2.4. MEASUREMENT OF HYDROPHILICITY FOR PLLA SCAFFOLDS.....	56
2.5. CELL ISOLATION AND CULTURE.....	56
2.6. SEEDING OF CELLS INTO SCAFFOLDS.....	57
2.7. VISUALIZATION OF CELL MORPHOLOGY.....	57
2.8. CELL VIABILITY ASSAY.....	58
2.9. ADHESION QUANTIFICATION.....	58
3. RESULTS	
3.1. HYDROPHILICITY OF PLLA AFTER PLASMA TREATMENT.....	59
3.2. CELL MORPHOLOGY AND DISTRIBUTION.....	59
3.3. CELL VIABILITY.....	63
3.4. ADHESION QUANTIFICATION.....	64
4. DISCUSSION.....	66
SUMMARY.....	69
CHAPTER 5: CONCLUSIONS.....	70
LITERATURE CITED.....	74

LIST OF TABLES

EFFECTS OF OXYGEN PLASMA TREATMENT ON HUMAN ADIPOSE-DERIVED ADULT STEM CELL ADHERENCE TO POLY(L-LACTIC ACID) SCAFFOLDS

Table 1. Effects of oxygen plasma treatment on cell adherence and spreading within melt-blown, non-woven PLLA scaffolds. (+/- = 0-10%; + = 10-30%; ++ = 30-60%; +++ = 60-100%).....	60
--	----

LIST OF FIGURES

THE EFFECTS OF REST INSERTED AND CONTINUOUS CYCLIC TENSILE STRAIN ON HUMAN ADIPOSE-DERIVED ADULT STEM CELL LINES DISPARATE OSTEOGENIC DIFFERENTIATION CAPABILITIES

RESULTS

Figure 1. Histochemical analysis of hADAS cells from two donors after osteogenically differentiated via chemical stimulation. Representative images of alizarin red-stained calcium deposits representing the osteogenic potential of A, B) Donor 1 (high calcium producer); C, D) Donor 2 (low calcium producer)..... 29

Figure 2. Calcium deposition of hADAS cells from donor 1 (high calcium producer) when cultured in osteogenic medium and exposed to one of the three loading conditions: continuous loading (10% strain, 1 Hz, 4 hrs), rest insertion loading (10% tensile strain, 1 Hz, 10 second rest insertion, 4 hrs), or unstrained..... 31

Figure 3. Calcium deposition of hADAS cells from donor 2 (low calcium producer) when cultured in osteogenic medium and exposed to one of the three loading conditions: continuous loading (10% strain, 1 Hz, 4 hrs), rest insertion loading (10% tensile strain, 1 Hz, 10 second rest insertion, 4 hrs), or unstrained..... 32

Figure 4. Proliferation of hADAS cells averaged from both donors when cultured in both osteogenic (OM) and growth medium (GM), measured as a percent reduction of alamarBlue™..... 33

EFFECTS OF OXYGEN PLASMA TREATMENT ON HUMAN ADIPOSE-DERIVED ADULT STEM CELL ADHERENCE TO POLY(L-LACTIC ACID) SCAFFOLDS

MATERIALS AND METHODS

Figure 1. A) Cross-section of fiber attenuation in the meltblowing process. Fibers are drawn and attenuated by hot air. B) Fibers are drawn, touch one another and self bond before being collected on the conveyor belt..... 54

Figure 2. SEM picture depicting morphology of non-woven PLLA scaffolds..... 55

RESULTS

Figure 3. Effects of oxygen plasma treatment of PLLA scaffolds on cell spreading. Representative images of hematoxylin-stained adipose-derived adult stem cells depicting

cellular morphology on untreated (A, C, E) or oxygen plasma treated (B, D, F) melt-blown, non-woven PLLA scaffolds at 2 (A, B), 4 (C, D), and 24 (E, F) hours after cell seeding. Scale bar = 20 μm 61

Figure 4. Effects of oxygen plasma treatment of melt-blown, non-woven PLLA scaffolds on the distribution of human adipose-derived adult stem cells throughout the construct. Representative images of hematoxylin-stained cells within two representative areas of an untreated (A, C, E) or an oxygen plasma treated (B, D, F) scaffold at 2 (A, B), 12 (C, D), and 24 (E, F) hour post-seeding. Scale bar = 20 μm 62

Figure 5. Effects of oxygen plasma treatment of PLLA scaffolds on cell viability. Representative images of human adipose-derived adult stem cells seeded on untreated (A, C, E) and oxygen plasma treated (B, D, F) PLLA scaffolds stained with calcein AM (green) and ethidium homodimer-1 (red, arrows) to label live and dead cells, respectively, at 2 (A, B), 24 (C, D), and 48 (E, F) hours post-seeding. Scale bar = 10 μm 63

Figure 6. The number of cells that adhered over 48 hours to untreated and oxygen plasma treated PLLA scaffolds based on DNA analysis for all three donors, represented individually and averaged together. Data represent the mean \pm SD..... 65

CHAPTER 1: INTRODUCTION AND LITERATURE REVIEW – BONE STRUCTURE, BIOMECHANICS, AND STEM CELLS

1. BONE

Bone is composed of an organic matrix (collagen) strengthened by deposits of calcium phosphate crystals. Ninety-five percent of the organic matrix consists of type 1 collagen and the remaining five percent is made up of proteoglycans and other noncollagenous proteins [1, 2]. The crystalline deposits within the matrix are primarily calcium and hydroxyapatite. Bone serves multiple functions within the body such as: 1) protection of vital organs, 2) support and attachment to muscles for locomotion, 3) generation of red and white blood cells for immunoprotection and oxygenation of other tissues, and, 4) mineral storage and ion homeostasis [2-4]. The physical properties of bone reflect the many roles that it serves in the body.

Structure

The adult skeleton consists of cortical bone (80%) and cancellous (or trabecular) bone (20%) [4]. Cortical bone is almost completely solid, having very low porosity (10%), whereas trabecular bone is loosely organized and very porous (50-90%) [2, 5]. This difference in porosity and arrangement are related to their primary functions: cortical bone provides mechanical stability and protection, having an ultimate compressive strength and modulus of elasticity ten times greater than that of trabecular bone [4]; metabolic functions take place within trabecular bone [2].

Cortical and trabecular bone consist of woven or lamellar bone, although woven bone is usually found in the embryonic skeleton and is eventually replaced by lamellar bone during maturation [5]. Woven bone has an extremely high rate of deposition and turnover, is composed of an irregular pattern of collagen fibrils, and contains four times as many osteocytes as lamellar bone. Lamellar bone is laid down much more slowly and is less mineralized than woven bone [1, 4]. The collagen fibrils in lamellar bone lie in tightly organized parallel sheets to form distinct lamellae, all oriented in one direction, that vary in thickness between 1-5 mm [1]. These lamellae can be oriented differently depending on location. Lamellae can be stacked along a flat surface or form concentric layers around a blood vessel. These concentric lamellae surround central canals and form osteons [5]. The central canals of osteons, or haversian canals, contain blood vessels, lymphatic vessels, and nerves. It is these canaliculi that provide the delivery of nutrients and waste removal for cells.

Bone Cells and Remodeling

Bone is comprised of four main classes of cells: bone-lining cells, osteocytes, osteoblasts, and osteoclasts [2, 4, 5]. Of these four cell types, bone-lining cells, osteoblasts and osteoclasts are found on the surface of bone whereas osteocytes penetrate through the entire mineralized interior. Either physical connections or chemical signaling between each type of cell is responsible for the dynamic remodeling of bone.

Osteoblasts are the fully differentiated cells responsible for the formation of new bone [2, 5]. They secrete type 1 collagen and the noncollagenous proteins that comprise the organic part of the mineralized matrix. During the formation of bone, their cytoplasmic processes extend through the bone matrix and interact with osteocytes. It is through these

connections that communication is made between osteocytes and osteoblasts to initiate the process of bone remodeling [4]. In addition, systemic hormones may also stimulate osteoblasts to activate osteoclasts [5]. After bone formation, osteoblasts may choose one of three courses: they may revert to an inactive osteoblast and remain on the surface of the bone, they may surround themselves with matrix and transform into osteocytes, or they can migrate away from the site of bone formation. Besides the formation of bone, these cells may also play a role in controlling electrolyte fluxes between extracellular fluid and osseous fluid and may influence the mineralization of bone through the synthesis of organic matrix components of bone and the production of matrix vesicles.

Osteocytes, or a mature osteoblast, make up 90% of bone cells found in the mature human skeleton [5]. The lacunae contain the cell body of the osteocytes but their cytoplasmic extensions extend throughout the entire mineralized bone matrix, via the canaliculi [6]. Connections are made with other osteocytes and osteoblasts via their cytoplasmic processes and communication between other osteocytes is done by gap junctions [2]. Due to the extensive network of osteocytes and bone-lining cells extending over and throughout the bone matrix, it is believed that these cells are responsible for “sensing” external loading and initiating the bone remodeling process [5]. However, there is evidence that osteocytes may also play a limited role in matrix production [6]. Possible theories are that they: 1) are involved in the maturation and mineralization of the osteoid matrix by secreting specific matrix molecules; or, 2) that they calcify the osteoid matrix by phosphorylating certain matrix components. Although they may be involved in mineralizing the bone matrix, they must also inhibit mineralization of the immediate matrix surrounding them in order to ensure diffusion of oxygen, nutrients, and waste removal.

Bone-lining cells (or surface osteocytes) have an elongated shape and are found directly along the surface of the bone matrix. Their cytoplasmic extensions penetrate the bone matrix and connect to each other and osteocytes via gap junctions [7]. When bone-lining cells are exposed to parathyroid hormone, they secrete enzymes which remove the thin lining (osteoid) covering the matrix to allow osteoclasts to begin resorption of bone.

Osteoclasts, the final class of bone cells, are responsible for the resorption of bone during the remodeling process [4, 5]. When osteoclasts degrade the bone, they create an acidic environment between the cell and the bone surface, called the sealing zone, and solubilize the mineral [5, 8]. This mechanism of lacunar acidification is achieved by the presence of V-type ATPase proton pumps in the ruffled border of the osteoclast [8]. To break down the remaining organic matrix, osteoclasts secrete acid proteases and/or may phagocytize any residual fragments. Once osteoclasts conclude the resorption of bone, they are thought to follow one of two routes: 1) osteocytes can be active in more than one bone resorption cycle or 2) are removed via apoptosis [8].

Mechanics of Bone

Mechanical loading of bone is translated into either strain, a small deformation of the calcified matrix, or fluid shear stress produced by interstitial fluid in the osteocyte canaliculi [9]. When bone is loaded, both bending and compression forces create degrees of strain on the bone surface [10]. Concurrently, the osteocytes and bone-lining cells are stretched to the same degree as the bone; however, the mechanical stretch on osteocytes will be biaxial due to a slight contraction of bone in the perpendicular direction [10]. The tensile strain imposed on the osteocytes and bone-lining cells causes a change in the shape of the cytoskeleton and

may, in turn, induce stretch-activated ion channels [10, 11], voltage sensitive channels via an influx of calcium and shift in membrane potential [10, 12], and stretch-activated cation channels [10].

The second method by which bone cells are externally loaded is an indirect result of matrix strain. When bone is loaded, the resulting compressive strain causes an increase in interstitial fluid pressure, forcing the fluid to flow to regions of low pressure [9, 13]. On a macro scale, this interstitial fluid flows through the lacuno-canalliculi and along the osteocyte processes [14]. However, because the matrix is so stiff, the deformation by physiological loads (on the order of 0.2%) is very small [7, 15]. This leads to the canalicular fluid flow hypothesis which proposes that these small strains impose a local force that initiates fluid flow between thin layers of non-mineralized matrix surrounding the osteocytes' bodies and processes, thus creating a shear stress (8-30 dynes/cm²) at the osteocyte cell membrane [16].

Bone Mechanotransduction

Osteocytes and bone-lining cells are presently thought by some investigators to be the primary mechanosensory cells responsible for interpreting mechanical forces and translating them to osteoblasts and osteoclasts for bone remodeling [4, 9, 14, 17]. Evidence to support the important mechanosensory role that osteocytes play in bone formation has been provided by multiple investigators [18-21]. Osteocytes have been found to be more mechanically sensitive to pulsatile fluid flow (PFF) than osteoblasts and periosteal fibroblasts, evident by an increase in prostaglandin E₂ (PGE₂), a potent stimulator for bone formation [14], by osteocytes but not by osteoblasts or periosteal fibroblasts [20]. These findings have been further validated by increased nitric oxide (NO) production by osteocytes in response to PFF,

with increases not being exhibited by periosteal fibroblasts [21]. Chicken osteocytes increased NO, which is linked to PGE₂ production [14], production by 2-fold after exposure to PFF, whereas periosteal fibroblasts exhibited no change in NO production in response to PFF. These studies provide convincing preliminary evidence that osteocytes are highly mechrosensitive cells capable of sensing mechanical deformation *in vivo*.

There are many possible mechanisms by which bone cells interpret external mechanical loads and transmit them via biochemical signals. One such method involves the extracellular matrix-integrin-cytoskeleton network [10, 19, 22]. Cellular tensegrity predicts that cells use their cytoskeleton to create an internal tension that stabilizes the cell shape, and that any reorganization of the cytoskeleton via external loading must first overcome this internal prestress [10, 23]. Transmission of mechanical stimulation across the cell surface is modulated by transmembrane receptors (i.e. integrins, CAMs, cadherins) that connect the cytoskeleton to an external substrate [23]. This connection provides a molecular pathway for mechanical signals to be passed across the cell surface, allowing these focal adhesion molecules to act as mechanoreceptors.

The transmission of mechanical signaling via the connection between integrins and the cytoskeleton have been linked to intracellular pathways that dictate cell viability [24], proliferation [25-27], morphology [24, 27], and differentiation [18, 25, 26, 28]. Chicken bone cells were used to demonstrate the relationship between the cytoskeleton and differentiation by evaluating PGE₂ expression when these cells were treated with or without an actin-filament disrupting agent and subjected to pulsatile fluid flow [19]. Typical fluid flow-induced differentiation of these cells was prevented when cells were treated with this actin-filament disrupting agent, indicative of the actin-cytoskeleton involvement in

mechanotransduction. The function of the actin cytoskeleton was further validated by Pavalko *et al.*, reporting that pulsatile fluid flow resulted in fluid shear stress-induced reorganization of the actin-cytoskeleton with concurrent increases in cyclooxygenase (COX-2) and c-Fox expression, both important in mechanically induced bone formation [29]. When fluid shear-induced stress fibers and focal adhesion formation was blocked by culturing the cells in an actin-filament disrupting agent (cytoschalasin B), COX-2 and c-Foc expression was inhibited. Together, these results demonstrate the critical role that actin stress fibers and their anchorage to the substrate via focal adhesions have on the mechanotransduction of external mechanical loads and subsequent bone formation.

Mechanically sensitive channels such as stretch activated ion channels [30-33], L-type voltage sensitive calcium channels[30, 34], and potassium-selective channels also play a role in mechanotransduction signaling. Evidence to support the important role that these mechanically sensitive channels play in mechanotransduction was provided by Rawlinson *et al.* It was demonstrated that the activation of stretch/shear-sensitive nonselective cation channels and L-type voltage-dependent calcium channels, in response to tensile strain of rat ulnae, are involved in osteogenic potential and metabolic activity [30]. Early production of prostanoids (PGE2 and PGI2), NO, and glucose-6-phosphate dehydrogenase activity were dependent on functional ion channels in bone cells. Specifically, strain-related responses in osteocytes primarily involve stretch/fluid shear cation channels. In contrast, strain-related responses in osteoblasts appear to involve both stretch/fluid shear cation channels and L-type voltage-dependent calcium channels. The role of mechanically sensitive channels were further confirmed by Li *et al.*, who demonstrated that blocking L-type voltage-sensitive calcium channels *in vivo* significantly, but not completely, suppresses the mechanical

loading-induced increase in mineralizing surface, mineral apposition rate, and bone formation rate [34]. Therefore, it is apparent that these calcium channels are significantly involved in bone adaption *in vivo*.

Transmission of mechanical signaling in bone cells to one another for the initiation of bone formation has been suggested to occur via a gap junctions. Osteocytes are connected to other osteocytes, bone-lining cells, osteoblasts, and osteoclasts through a network of gap junctions [4, 35, 36]. Evidence that osteocytes detect and communicate mechanical signals to osteoblasts via gap junctions was obtained in a study performed by Taylor *et al.* [36]. Osteocytes and osteoblasts were cocultured under conditions that allowed for gap junction intercellular communication. When osteocytes were exposed to a fluid shear stress of 4.4 dynes/cm², osteoblasts responded with a rapid and significant increase in alkaline phosphate (AP) activity. However, this increase was not evident when osteoblasts were directly exposed to fluid shear stress, indicative that osteoblasts respond to mechanical load through communication from osteocytes via gap junctions.

2. STEM CELLS

Stem cells are defined as self renewing cells capable of extensive proliferation and terminal differentiation [37, 38]. Traditional stem cells are considered an embryonic population of cells that undergo further development as the organism matures. The purpose of these cells is to replenish a diminished population of differentiated cells that for some reason cannot proliferate themselves. However, as embryogenesis continues, embryonic stem cells give rise to multipotent cells that are then only able to regenerate certain types of tissue [39]. Because this may encompass many different types of tissues, this brings about subclasses of stem cells in the adult body that are optimal for the terminal differentiation of specific tissues. The first defined class of adult stem cells was identified by Maximov in the early 1900s as being adult hematopoietic stem cells, which give rise to cells found in the blood. Over the years, other subclasses of adult stem cells have been isolated in the bone marrow such as those for endothelial, epithelial, muscle, liver, nerve, and mesenchymal tissue [39]. These adult stem cells are more readily available than embryonic stem cells and have the potential to provide tissue replacement or regeneration for a wide range of applications.

Mesenchymal Stem Cells

Mesenchymal stem cells (MSCs) are defined as progenitor cells which have the ability to differentiate into tissues of a mesenchymal lineage such as bone, cartilage, adipose, tendon, muscle, ligament and stroma [40]. These cells can be isolated from bone marrow [40, 41], umbilical cord blood [42], peripheral blood [43], amniotic fluid [44, 45], and adipose tissue [46-49]. Typical characterization of mesenchymal stem cells consists of the expression

of specific protein markers such as, but not limited to, CD44, CD71, CD90, CD105, CD106, and CD166 [40, 50, 51], and their ability to differentiate down osteogenic [41, 47, 52-62], adipogenic [41, 47, 63, 64], chondrogenic [41, 47, 54, 65-68], fibrogenic [69-71], myogenic [47, 56, 72], and neuronal [41, 46, 56, 73] pathways via chemical and/or mechanical stimulation.

Sources of Mesenchymal Stem Cells

The majority of applications using stem cells for tissue or organ replacement typically use bone marrow-derived mesenchymal stem cells (BMMSCs) [53, 65, 70-72, 74-76]. However, the limited source of these cells constrains the feasibility of using them in large commercial applications. Researchers have begun to investigate other sources of mesenchymal stem cells, specifically from adipose tissue. In contrast to bone marrow-derived mesenchymal stem cells, adipose tissue is an abundant and easily obtainable source of cells [77]. In a study performed by De Ugarte *et al.*, adipose derived adult stem (ADAS) cells showed the same capacity for expansion, growth kinetics, and differentiation as that of BMMSCs [41]. Other studies involving ADAS cells have shown their multipotentiality by inducing these cells down osteogenic, myogenic, adipogenic, and chondrogenic lineages [41, 46, 47, 55, 60, 78]. However, the use of ADAS cells as a substitute for BMMSCs in certain applications has stimulated controversy due to inconsistent reports of ADAS cell differentiation potential.

While some investigators have reported that there are no differences between the potential for BMMSCs and ADAS cells to differentiate down multiple pathways [41, 63, 78], others report that ADAS cells are inferior to BMMSCs with respect to their ability to

differentiate down certain lineages [47, 54, 67, 68, 79, 80]. De Ugarte *et al.* examined the multi-lineage potential of bone marrow-derived MSCs to ADAS cells and found that under chemical stimulation, there was no difference between the two cell types in their ability to undergo osteogenic and adipogenic differentiation, express neuron-like morphology, or show differences in growth kinetics [41]. Likewise, Hattori *et al.* was able to confirm that both BMMSCs and ADAS cells cultured in osteogenic medium are able to express similar quantities of calcium phosphate deposition and osteocalcin secretion. However, studies done by Im *et al.* and Mehlhorn *et al.* argue that these two cell types do not have the same potential to differentiate down osteogenic or chondrogenic lineages. Im *et al.* found that AP activity in BMMSCs was significantly greater than ADAS cells after 2 and 3 weeks, as well as the level of mineralization [54]. In addition, chondrogenesis was found to be greater with BMMSCs, evident by safranin-O staining and immunohistochemical staining for type II collagen, compared to ADAS cells. The results of a study by Mehlhorn *et al.* looking at chondrogenesis agreed with this study. BMMSCs, cultured in TGF- β 1 supplemented medium, showed an increase of collagen type II, type X, cartilage oligomeric matrix protein, and aggrecan mRNA expression 3-15 times higher than ADAS cells [67].

While all of these studies lead to a suspicion that ADAS cells are inferior to BMMSCs in differentiation potential, it is important to note that these comparisons were done under the same media conditions, specifically, media conditions optimized to promote differentiation of BMMSCs. Other distinctions between ADAS cells and BMMSCs such as expressing different surface markers [47, 50], requiring additional medium supplements to differentiate down specific lineages [81, 82], and upregulation in different genes during differentiation [80] all lead toward a possibility that ADAS cells are, in fact, not inferior but

just behave differently than BMMSCs. Therefore, before judgment is made on the potential use of ADAS cells in tissue engineered organs, a better understanding of ADAS functionality is needed.

Mesenchymal Stem Cells for Tissue Engineering

The potential for MSCs to be a viable substitute for embryonic stem cells in specific applications of tissue regenerative medicine has opened up many opportunities in tissue and organ engineering. Traditional methods of dealing with degenerative skeletal diseases and wounds are to use allografts, autografts, or artificial implants. However, these techniques are not ideal because of possible donor site morbidity, low tissue availability, immunogenic responses or loosening of implants [83-86]. The use of the patient's own mesenchymal stem cells for treatment, on the other hand, do not induce any immunogenic response and are in greater supply. Because of these advantages, MSCs are being greatly investigated for applications in tissue regeneration and/or remodeling. Two components to consider for tissue engineering transplants are: 1) tissue-specific cells; and, 2) a biocompatible scaffold to which the cells can adhere and that provides short-term mechanical stability until the cells produce an extracellular matrix in the defective site [84, 87, 88]. Researchers and physicians have utilized these components in: 1) bone [53, 74-76, 89, 90]; 2) cartilage [65, 91-94]; and, 3) tendon [70, 95, 96] repairs.

Bone repair is of great importance in the tissue engineering field. Autologous bone grafts are usually used in clinical cases but often present additional problems in terms of adequate quantities of donor tissue and potential donor morbidity. Instead, the use of MSCs combined with a biocompatible scaffold has become a novel approach for treatment or tissue

replacement. An early study by Bruder *et al.* demonstrated that bone marrow-derived MSCs loaded into scaffolds consisting of hydroxyapatite and β -tricalcium phosphate ceramic could be used to treat a large defect in the femora of adult female dogs [76]. Their study consisted of three groups: Group A contained dogs treated with MSC-loaded scaffolds, dogs in Group B were given scaffolds with no cells loaded into it, and the defects in the dogs of Group C were not treated at all. Results of this study showed that union occurred more quickly in defects treated with hMSC-seeded scaffolds than all other conditions, with a large osseous callus developing around five of the six implants and the adjacent host bone. In addition, more bone filled the pores of the hMSC-seeded scaffold compared to other groups.

Kon *et al.* was able to use the same method of filling a porous hydroxyapatite ceramic scaffold with autologous BMSCs to repair a critical-size bone defect in sheep [90]. Upon retrieval of cell-seeded constructs and unseeded constructs 2 months post implantation, bone formation around and throughout the porous scaffold was higher in BMSC-seeded scaffolds as compared to controls (54.2% and 8.6%, respectively). Their investigation also tested the mechanical properties of loaded and unloaded scaffolds and found that cell-loaded specimens had a higher stiffness compared with cell-free scaffolds.

The success of using BMSC-seeded scaffolds in animal models led to the first human clinical trial to repair critical-size bone defects by Quarto *et al.* [89]. Three patients were treated with bone grafts comprised of BMSCs seeded on HA scaffolds, representative in size and shape to their injury. Using radiographs and computed tomography scans, callus formation along the implants and integration at the interfaces with native bone was observed 2 months after surgery. By 13 months post surgery, all external fixations at the site of injury,

originally supplied for mechanical stability, were removed and patients had not reported any problems.

Differentiation via Chemical Stimulation

As tissue engineering technology continues to progress, new methods have been developed to successfully provide tissue replacements. Advances in this technology have utilized *in vitro* expansion of MSCs and induction of differentiation prior to implantation into the defective site. One way of differentiating human mesenchymal stem cells (hMSCs) is by chemical stimulation [46, 53, 97, 98], using growth factors to induce lineage specific differentiation. Osteogenesis can be obtained by treating MSCs with dexamethasone [97-100] or BMP-2 [99, 101]; typical adipogenic medium for bone marrow-derived hMSCs uses 1-methyl-3-isobutylxanthine, dexamethasone, insulin, and indomethacin [40]; chondrogenic differentiation has been achieved in bone marrow-derived MSCs by adding transforming growth factor- β 3 to serum free medium [40].

Differentiated cells are characterized for histological markers, protein and gene markers, and morphological properties specific to each lineage. Histological staining is typically applied in the characterization of osteogenic, adipogenic, and chondrogenic differentiation by the appearance of calcium deposits (Alizarin Red), sulfated proteoglycan matrix (Alcian Blue), and intracellular lipid-filled droplets (Oil Red O), respectively [40, 47, 51, 80]. Osteogenesis can also be quantified by the upregulation of bone markers such as bone morphogenetic protein-2, COL I, alkaline phosphatase, osteocalcin, and osteopontin [40, 47, 51, 60, 102].

Differentiation via Mechanical Stimulation

While these methods of differentiation via chemical components are generally effective, studies including mechanical stimulation [52, 103-106] are proving to be more appropriate based on information gathered about native stresses that these cells naturally experience *in vivo*. For example, ligament and tendon fibroblasts are repeatedly experiencing mechanical loading under normal physiological conditions. During the normal healing process, ligament remodeling stimulates the production of type I and type III collagen by certain growth factors, particularly that of TGF- β 1 in ligament fibroblasts. Kim *et al.* showed that type I and type III collagen gene expression and TGF- β 1 secretion were all up-regulated after applying uniaxial cyclic stretch to human anterior cruciate ligament cells [107]. Likewise, tendon fibroblasts appear to respond positively when undergoing uniaxial mechanical stretching, with an increase in cell proliferation and mRNA expression of collagen type I and TGF- β 1 [69]. As opposed to stretch, chondrogenic differentiation seems to be induced by compressive forces. Saitoh *et al.* used MSCs from rats to show that the level of chondrogenic differentiation marker expression increased with increased compression forces [66].

The role of mechanical stimulation in the differentiation of human mesenchymal stem cells (hMSCs) down an osteogenic pathway, in particular, has received notable attention. It has long been understood that bone remodeling is sensitive to external loading. The original idea that mechanical loading is responsible for the architecture of bone is credited to Julius Wolff's mathematical equations developed in the 19th century [108]. Wolff's Law states that the architecture of bone will adapt to an increase or decrease in loading by remodeling itself through a feedback system [109]. These ideas were expanded further by Harold M. Frost,

who proposed that a minimum effective strain (MES), or “setpoint,” determines the remodeling process [110]. If bone strains rise above the MES, remodeling occurs to increase bone mass; a bone strain below the MES retards bone remodeling.

The “mechanostat” hypothesis proposed by Henry Frost is also supported by the response of osteocytes *in vivo* due to mechanical loading. It has been well documented that the bone remodeling process is initiated by the sensing of mechanical stimuli, either as strain or fluid-induced shear stress, by osteocytes which in turn signal osteoblasts to form the bone matrix. By applying what is understood of physiological conditions, it is reasonable to deduce that the same mechanical stimulation may play a role in the differentiation of mesenchymal stem cells down an osteogenic pathway.

Utilizing the principle of mechanically stimulating bone formation, uniaxial tensile strain has been used successfully to induce bone regeneration via distraction osteogenesis [108, 111-114]. In a study utilizing rat models, Lobo *et al.* reported that gradual distraction of the mandible (0.25mm every 12 hours) over 8 days, followed by 28 days of rest resulted in periosteal bone formation by postoperative day (POD) 7 and a full bridge of new bone spanning the width of the distraction gap by POD 41 [111]. A similar study done by Meyer *et al.* reported that distraction osteogenesis of the mandible under physiological magnitudes (2000 microstrain) resulted in woven bone formation and some lamellar ossification after 14 days. Over the same time period, a magnitude of 20,000 microstrains resulted in thin trabecular bone formation over the entire gap and active osteoblasts could be seen on a layer of primary bone [108].

Cyclic tensile strain has also been successful in inducing osteogenesis of bone marrow-derived hMSCs *in vitro* [52, 57, 58, 115]. Sumanasinghe *et al.* found that even in the

absence of osteogenic differentiation medium (i.e. cells maintained in complete growth medium) 10% strain, 1 Hz, for 4 hours resulted in an upregulation of BMP-2 in hBMSCs seeded in a three-dimensional collagen matrix after 1 week, a significant 4-fold increase over unstrained samples [52]. Likewise, Ignatius *et al.* reported that cyclic tensile strain (1% at 1 Hz for 1800 cycles/day) for 3 weeks resulted in slight increases of histone H4, alkaline phosphatase, core binding factor 1, and osteopontin compared to unstrained controls [116]. Characteristics such as magnitude [52], number of cycles [117], and frequency [117] of strain have been shown to be important variables for optimal tissue regeneration.

Rest Insertion Loading

These previous studies investigating mechanical loading-induced osteogenesis have been performed under continuous strain. More recently, the duration of continual strain has come under scrutiny. Qin *et al.* [118] and Rubin *et al.* [15] both described a nonlinear correlation between duration of loading and differentiation, each reporting a threshold for number of loading cycles when attempting to regulate bone mass in the ulnae of turkeys and roosters, respectively. In the case of applying a 0.5 Hz compression loading to the ulnae of mature roosters, the optimal loading regimen for bone mineral content was 36 loads per day [15]. When the number of loads was increased to 360 or 1800 loads per day, the amount of bone deposited or the character of the bone during remodeling did not increase. In addition, progression of bone mineral content stabilized at 28 days of loading and actually decreased when loading was continued for 5 or 6 weeks. This response of “diminishing returns” [119] was also demonstrated in rats when trained to perform a specific number of jumps per day. When rats underwent five jumps per day at a height of 40 cm, the bone mass and breaking

force was greatly improve when compared to controls [120]. However, this result was not greatly amplified when the number of jumps per day was increased to 10, 20, or 40. These findings indicate that large numbers of strains per day is unnecessary for significant *in vivo* bone growth in rats. Both of these studies illustrate two key mechanisms that were first defined by C. H. Turner [119]: 1) only a short loading regimen is required to maximize bone formation, and 2) a longer loading session does not increase the osteogenic effects.

In an attempt to integrate these phenomena, researchers have begun to insert rest periods between loading cycles in an effort to restore mechanosensitivity in cells and therefore optimize the osteogenic effects of mechanical loading. The effects of both long recovery periods (hours) and short-term recovery periods (seconds) have been investigated to restore mechanosensitivity in desensitized cells both *in vivo* [121-126] and *in vitro* [127, 128]. In a study performed by Robling *et al.* on rat tibias, eight hours of recovery between loading bouts was sufficient to return the cells to their original mechanosensitivity level, evident by the 125% increase in relative bone formation rate, compared to animals that did not receive any recovery time between loading bouts [121]. Results from a short-term recovery experiment within the same study revealed that although bone remodeling was significantly enhanced by applying rest insertions in between loading cycles, there was no significant difference in the results between the 0.5, 3.5 and 7 seconds recovery groups. However, the improvement in relative mineralizing surface and relative bone formation rates were significantly greater (66-190%) in the 14 seconds recovery group compared to the other recovery groups. This last finding indicates the existence of a recovery threshold that must be surpassed in order to obtain significant increases in osteogenesis. This time scale is similar to results found when cyclic mechanical loading was applied to the right tibiae of female mice

[122]. Bone formation response was greater when 10 seconds of rest was inserted between loading cycles compared to loading regimens without rest periods between cycles. In addition, the osteogenic response to mechanical loading continued as the number of loading cycles in each bout increased only when 10 seconds of rest was inserted between cycles, suggesting that inserting rest periods counters the phenomenon of “diminishing returns.”

Not only have studies involving the addition of rest periods between loading regimens been performed *in vivo*, but recent investigations have found similar results in osteoblasts *in vitro*. In a study involving intracellular calcium signaling within rat osteoblastic cells, investigators found that cells did not usually respond to additional fluid-flow loading bouts [128]. However, when cells were allowed a rest period of at least 10 minutes, the number of cells that responded to a second loading bout significantly increased and a 15 minute rest period was required to regain the same magnitudes of internal calcium measured after the initial bout of fluid flow [128]. Another study investigating fluid-induced signaling in mouse osteoblastic cells found that a rest period of 10 and 15 seconds inserted in oscillatory fluid flow regimens significantly increased the concentration of intercellular calcium produced in cells, the number of cells that responded to the mechanical loading, and the percentage of cells that responded to the fluid flow more than once [127]. However, when the shear stress applied to the osteoblasts during fluid flow was decreased from 2 Pa to 1 Pa, loading regimens that incorporated a 10 second rest period had a much higher increase in intracellular calcium production and in the number of cells to respond to the mechanical loading compared to both the control and 15 second experimental group. Results from these rest insertion loading studies imply that a more optimal loading regimen exists for mechanically-induced osteogenesis. It is the focus of this thesis to evaluate the response to rest insertion

loading compared to continuous loading of human adipose-derived adult stem (hADAS) cells from two donors exhibiting high and low calcium deposition capabilities; and to increase hADAS cell adherence to three-dimensional poly(L-lactic acid) (PLLA) scaffolds using oxygen plasma treatment for the eventual use of *in vivo* implantation.

To accomplish these goals, the following chapters present two studies that examine the mechanobiology of hADAS cells in response to cyclic tensile strain and their adhesion properties on PLLA. In Chapter 2, I present analysis of continuous and rest inserted cyclic tensile strain on hADAS cells compared to continuously strained and unstrained samples of two donors which exhibit varying degrees of osteogenic differentiation capabilities. Chapter 4 examines the use of oxygen gas plasma treatment of PLLA in order to increase hADAS cell adhesion for possible future enhancement of cell proliferation and differentiation. Finally, Chapter 5 discusses the results of these two studies and their implications for future investigation.

CHAPTER 2. THE EFFECTS OF REST INSERTED AND CONTINUOUS CYCLIC TENSILE STRAIN ON HUMAN ADIPOSE-DERIVED ADULT STEM CELL LINES WITH DISPARATE OSTEOGENIC DIFFERENTIATION CAPABILITIES

A.D. Hanson, S.W. Marvel, S.H. Bernacki, A.J. Banes, and E.G. Lobo

The following chapter discusses the use of cyclic tensile strain to increase the osteogenic response of human ADAS (hADAS) cells. We are interested in the hADAS cell response to rest inserted and continuous cyclic tensile strain with respect to differentiation and proliferation. We are further interested in investigating the effects of mechanical loading on hADAS cell lines with unequal osteogenic differentiation capabilities.

1. INTRODUCTION

Mesenchymal stem cells (MSCs) have been utilized in many studies investigating the development of tissue engineered bone constructs [76, 89, 90]. These cells have been shown to readily differentiate under both chemical [97, 98, 100] and mechanical stimulation [52, 57, 58, 115]. However, in order to produce a tissue engineered bone construct with similar mechanical properties to native tissue, the proper combination of mechanical and chemical stimuli needs to be determined.

Early studies to investigate mechanically induced *in vivo* osteogenesis have used distraction to encourage bone growth between gaps in native bone [111-113, 129]. Recent studies in our lab have shown that human bone marrow-derived MSCs (hMSCs) in three-dimensional collagen constructs are also responsive to uniaxial tensile strain *in vitro*, evident by the upregulation of BMP-2 which is an early marker of osteogenesis [52]. While mechanical loading has provided insight into the mechanisms by which MSCs can differentiate, it has recently been discovered that mesenchymal stem cells and bone progenitor cells *in vitro* and *in vivo* will eventually become desensitized and thus unresponsive to continual mechanical loading [15, 118, 120]. Studies involving animal models revealed that not only is there a threshold for number of loading cycles before cells become desensitized [118, 121], but also that longer loading duration does not increase bone growth [120]; and may actually decrease bone mineral content [121]. These findings illustrate two key mechanisms in bone development: 1) only a short loading regimen is required to maximize bone formation; and, 2) a longer loading duration does not increase osteogenic effects [119].

In an attempt to integrate these phenomena, researchers have inserted rest periods between loading cycles in an effort to restore mechanosensitivity in cells and therefore optimize the osteogenic effects of mechanical loading. The effects of both long recovery periods (hours) and short-term recovery periods (seconds) have been investigated to restore mechanosensitivity in desensitized cells both *in vivo* [121-126] and *in vitro* [127, 128]. As investigators began evaluating several recovery times to optimize cells' response to mechanical loading, the existence of a recovery threshold was discovered [121]. Robling *et al.* found that when evaluating 0.5, 3.5, 7, and 14 seconds of rest between mechanical loading bouts on rat tibiae, improvements in relative mineralizing surface and relative bone formation rates were significantly greater when 14 seconds of rest was applied [121]. A rest period of greater than 7 seconds has been confirmed in two other studies, both *in vivo* using mice tibiae [122] and *in vitro* using osteoblasts [127]. In both of these studies, a rest period of 10 seconds was found to be optimal for counteracting the phenomenon of “diminishing returns.”

As stem cells become more widely used in developing tissue engineered bone constructs, the source of adult stem cells have come under scrutiny due to availability and application. Early investigations focused on using bone marrow-derived mesenchymal stem cells (MSCs) for tissue engineering bone constructs. Although these studies were successful in promoting MSCs down an osteogenic pathway [40, 57, 58, 102, 115], isolating bone marrow is a painful experience for patients and the amount of cells recovered is limited. Adipose-derived adult stem (ADAS) cells, an abundant and easily obtainable source of adult stem cells, have been shown to produce similar differentiation capabilities compared to bone marrow-derived MSCs [41, 55, 63] and therefore may be a better cell source for engineering tissue constructs in the future. However, while some investigators report that both ADAS and

bone marrow-derived MSCs can differentiate down multiple pathways [41, 47, 63, 78], other investigators have published data suggesting that MSCs have superior differentiation abilities over ADAS cells [54, 67, 68, 79]. One possible reason for these conflicting results is donor variability [64, 79, 130, 131], a phenomenon also experienced in our lab and reported in an earlier study [132]. Another reason for these results could be due to findings that ADAS cells require different medium supplements to differentiate down specific lineages than MSCs [81, 82, 133]. This, along with differences in surface markers [47, 50] and the upregulation of different genes during differentiation [80], all lead towards the possibility that ADAS cells behave differently than MSCs from different sources.

In this study, our objective was two-fold: 1) apply the lessons observed in the rest insertion studies with hMSCs described above to enhance the effects of tensile strain on osteogenic differentiation of human ADAS (hADAS) cells; and, 2) evaluate how tensile strain would affect osteogenesis of hADAS cells using hADAS cell lines with distinct osteogenic differentiation capabilities (i.e. one cell line exhibiting high calcium deposition in osteogenic differentiation medium and the other exhibiting low calcium deposition). Based on these objectives, we first hypothesized that by adding 10 seconds of rest between each loading cycle, the amount of calcium deposition by both hADAS cell lines would increase. We also hypothesized that mechanical loading, in general, would enhance osteogenesis of hADAS cells with reduced osteogenic potential.

2. MATERIALS AND METHODS:

2.1 Cell Isolation and Culture

Human ADAS cells were isolated from excess adipose tissue remaining from either abdominoplasty or liposuction procedures performed at UNC hospitals in accordance with an approved IRB protocol. Tissue samples were obtained from two female donors, ages 36 and 44. Cell isolation and characterization was performed as described earlier by our lab [51]. In brief, adipose tissue was digested in 0.075% collagenase type I (Worthington Biochemical Corp., Lakewood, NJ) for 30 minutes. Stromal cells isolated by digestion were then pelleted by centrifugation and resuspended in 160mM ammonium chloride to lyse remaining blood cells. Human ADAS cells were again sedimented by centrifugation for 10 minutes, resuspended in complete growth medium (minimum essential medium eagle, alpha-modified supplemented with 10% FBS (Atlanta Biologicals, Lawrenceville, GA, USA), 2 mM L-glutamine, 100 units/ml penicillin and 100µg/ml streptomycin), and plated in T-75 flasks. After 24 hours, the cell monolayer was washed with 1xPBS to remove nonadherent cells, and fresh growth medium was replaced. Once hADAS cells reached 70% confluency, cultures were washed twice with 1xPBS and cells removed from the flasks with 0.05% trypsin/0.53 mM EDTA. Cells were characterized by immunofluorescent staining for positive markers CD105 and CD166, and negative markers CD34 and CD45. All chemicals and supplies used in cell culture procedures were purchased from Mediatech (Herndon, VA, USA) and Gibco-BRL (Grand Island, NY, USA) unless otherwise noted.

Characterization of Osteogenic Differentiation Potential

Frozen samples of hADAS cells at passage two were thawed and plated at 1.3×10^3 cells/cm² in T-75 flasks. Once cells reached 70% confluency, cultures were washed twice with 1x PBS and cells were removed from flasks with 0.05% trypsin/0.53 mM EDTA. Human ADAS cells from each donor were seeded at 5.2×10^3 cells/cm² in nunclon-treated polystyrene 6-well tissue culture plates. Cells were cultured in complete growth medium until they reached 100% confluency. Once reaching 100% confluency, growth medium was replaced by either new growth medium or osteogenic medium (growth medium supplemented with 50 μ M ascorbic acid, 0.1 μ M dexamethasone, and 10mM β -glycerolphosphate). After cells were cultured in their respective media, each cell line was characterized for its osteogenic differentiation potential by staining for calcium deposits (Alizarin Red). To evaluate differentiation, digital light microscopy images were obtained from each stained culture (3 cultures/cell line), and the pixel area per field of view (3 fields/culture) covered by stained calcium deposits was determined by color-based image analysis using Adobe Photoshop (San Jose, CA, USA).

2.3 Seeding of Cells in Bioflex™ Culture Plates

Human ADAS cells from passage two were expanded in T-75 flasks and maintained in complete growth medium. Once cells reached 70-80% confluency, cells were trypsinized and seeded in Bioflex™ culture plates (Flexcell Int., Hillsborough, NC, USA) coated with collagen type I at a density of 50,000 cells per 2 ml complete growth medium. Cells were allowed to reach 100% confluency within the tissue culture plates before medium was changed to either fresh complete growth medium or osteogenic medium (growth medium

supplemented with 50 μM ascorbic acid, 0.1 μM dexamethasone, and 10 mM β -glycerophosphate). Samples were separated into experimental groups representing three loading regimens. Cells seeded in Bioflex® tissue culture plates were either exposed to continuous uniaxial cyclic tensile strain (n=6), rest inserted uniaxial cyclic tensile strain (n=6), or did not receive any loading (n=6).

2.4 Application of Mechanical Loading

Samples undergoing mechanical loading were subjected to 10% uniaxial cyclic tensile strain at 1 Hz for 4 hours per day using a Flexcell® Tension Plus™ System (Flexcell Int., Hillsborough, NC, USA). The two experimental groups exposed to tensile strain either underwent mechanical loading for 4 hours continuously or received a 10 second rest period in between each loading cycle (11 seconds per cycle). Control groups consisted of unstrained cells seeded in Bioflex® tissue culture plates.

2.5 Calcium Deposition

Osteogenesis was evaluated on days 1, 4, 7, and 14 by quantifying the amount of calcium mineral deposited by cells using StanbioTotal Calcium LiquiColor® (Stanbio Laboratory, Boerne, TX, USA). Cell monolayers were washed twice with 1xPBS, after which 1 ml of 0.5N HCl was added to each well. Human ADAS cells and HCl were removed from the wells and placed in microcentrifuge tubes to be stored in -20° until the assay was performed. Aliquots of 10 μl per sample were mixed with 200 μl of a color and base working reagent. The absorbance of the solution was read in a microplate reader (Tecan, Durham, NC, USA) at 550 nm and readings were normalized to values representative of known calcium

concentrations. Student's t-tests were used to determine significant differences ($p < 0.05$) in calcium deposition between all experimental regimens.

2.6 Cell Viability and Proliferation

Viability and proliferation of hADAS cells were evaluated at 1, 4, 7, 10, and 14 days using alamarBlue™ (BioSource Int., Camarillo, CA, USA). One hour after straining was completed, 200 μ l of alamarBlue™ was added to the 2 ml of medium in each tissue culture plate well. Cells were allowed to incubate for 1 hour, after which 100 μ l aliquots of the alamarBlue™ containing medium was removed from the wells and deposited in a 96 well plate. Samples were read using a microplate reader (Tecan) at wavelengths of 570 nm and 600 nm. Percent reduction of alamarBlue™ was calculated using the following equation [134]:

$$\% \text{ reduction of alamarBlue}^{\text{TM}} = \frac{(\epsilon_{\text{ox}})^{\lambda_2} A^{\lambda_1} - (\epsilon_{\text{ox}})^{\lambda_1} A^{\lambda_2}}{(\epsilon_{\text{RED}})^{\lambda_1} A'^{\lambda_2} - (\epsilon_{\text{RED}})^{\lambda_2} A'^{\lambda_1}} \times 100$$

Where: ϵ_{ox} = molar extinction coefficient of alamarBlue oxidized form (Blue)

ϵ_{RED} = molar extinction coefficient of alamarBlue oxidized form (Red)

A = absorbance of test wells

A' = absorbance of negative control well (media plus alamarBlue but no cells)

$\lambda_1 = 570\text{nm}$

$\lambda_2 = 600\text{nm}$

3. RESULTS

3.1 Calcium Deposition

The hADAS cell line from donor one was characterized as being able to deposit high amounts of calcium when cultured in osteogenic medium while the hADAS cell line from donor two was distinguished as able to deposit low amounts of calcium (Figure 1). Using histochemical staining for lineage-specific calcium deposition, donor one showed a 2-fold increase in its ability to differentiate down the osteogenic pathway compared to donor two (data not shown).

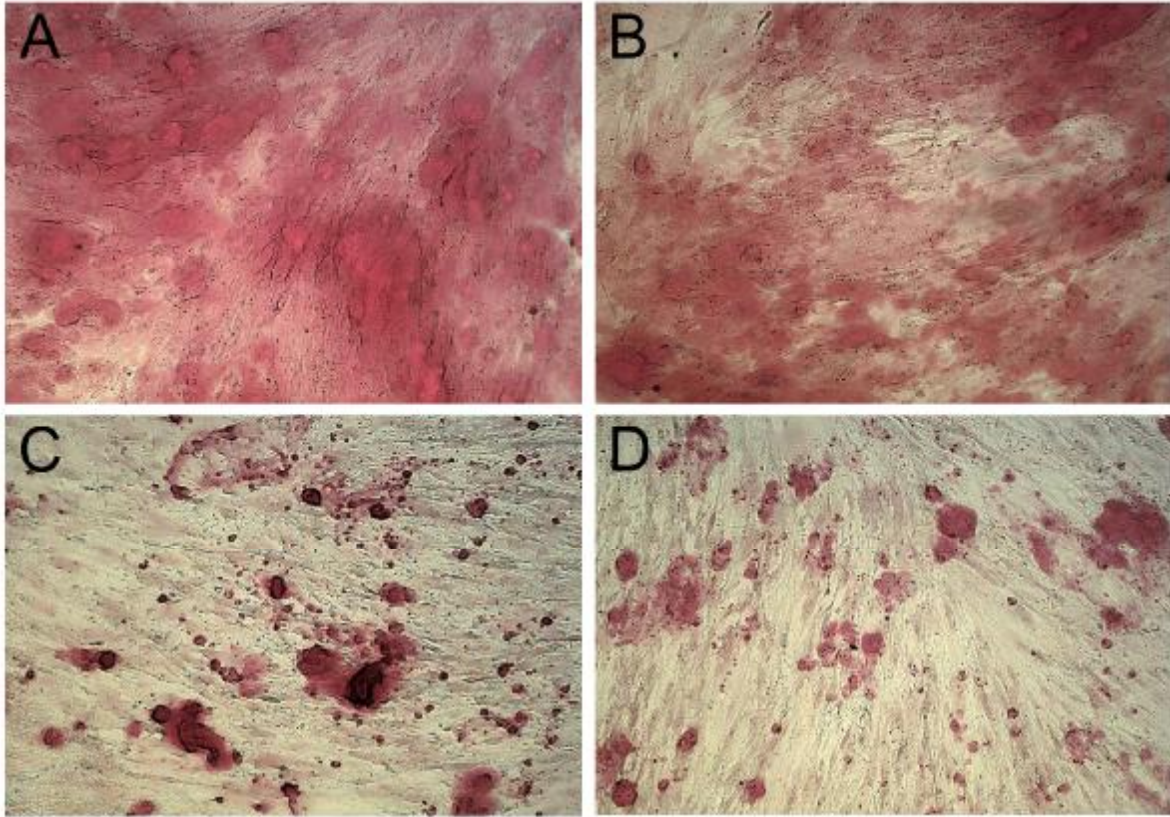


Figure 1. Histological analysis of hADAS cells from two donors after osteogenically differentiated via chemical stimulation. Representative images of alizarin red-stained calcium deposits representing the osteogenic potential of A, B) High calcium deposition hADAS cell line (donor 1); C, D) Low calcium deposition hADAS call line (donor 2). Photographs were taken at 10x.

The high and low calcium deposition hADAS cell lines each exhibited increased calcium deposition in response to mechanical stimulation, both continuous and rest insertion loading, as compared to hADAS cells in static (unstrained) culture (Figures 2, 3). Early time points (days 1 and 4) did not yield physiologically significant amounts of calcium deposition from either cell line (Figures 2, 3).

Human ADAS cell line with high calcium deposition capabilities:

Human ADAS cells from donor one, cultured in osteogenic medium, increased calcium deposition on day 7 to $0.075 \mu\text{g}/\text{cm}^2$ under continuous loading, $0.035 \mu\text{g}/\text{cm}^2$ with rest insertion, and $0.017 \mu\text{g}/\text{cm}^2$ when unstrained (Figure 2). By 14 days, hADAS cells exposed to continuous loading deposited an average of $0.415 \mu\text{g}/\text{cm}^2$ of calcium, $0.441 \mu\text{g}/\text{cm}^2$ with rest insertion, and $0.158 \mu\text{g}/\text{cm}^2$ when unstrained. Although rest insertion loading did not result in a significant increase in calcium deposition compared to continuous loading, both loading conditions did result in a significant increase compared to unstrained controls ($p < 0.01$).

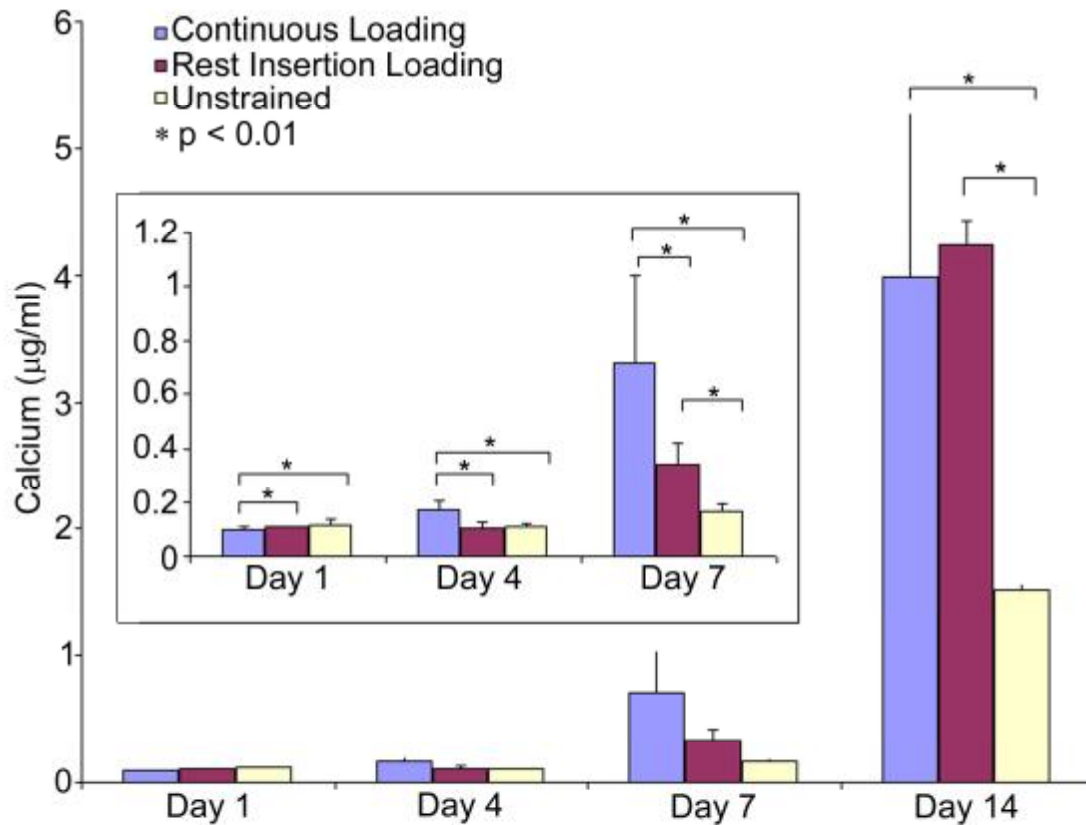


Figure 2. Calcium deposition of hADAS cells from donor 1 (high calcium deposition). Human ADAS cells cultured in osteogenic medium and exposed to one of the three loading conditions: continuous loading (10% strain, 1 Hz, 4 hrs), rest insertion loading (10% tensile strain, 1 Hz, 10 second rest insertion, 4 hrs), or unstrained.

Human ADAS cell line with low calcium deposition capabilities:

The hADAS cells cultured in osteogenic medium did not yield physiologically significant quantities of calcium until day 14. Measurements at day 14 showed an average of 0.251 $\mu\text{g}/\text{cm}^2$ calcium for cells strained continuously, 0.237 $\mu\text{g}/\text{cm}^2$ with rest insertion, and 0.171 $\mu\text{g}/\text{cm}^2$ in static culture (Figure 3). Similar to the high calcium depositing hADAS cell line, cells which underwent rest insertion loading did not deposit more calcium than those

strained continuously, but calcium measurements for both loading conditions were significantly higher than unstrained cells.

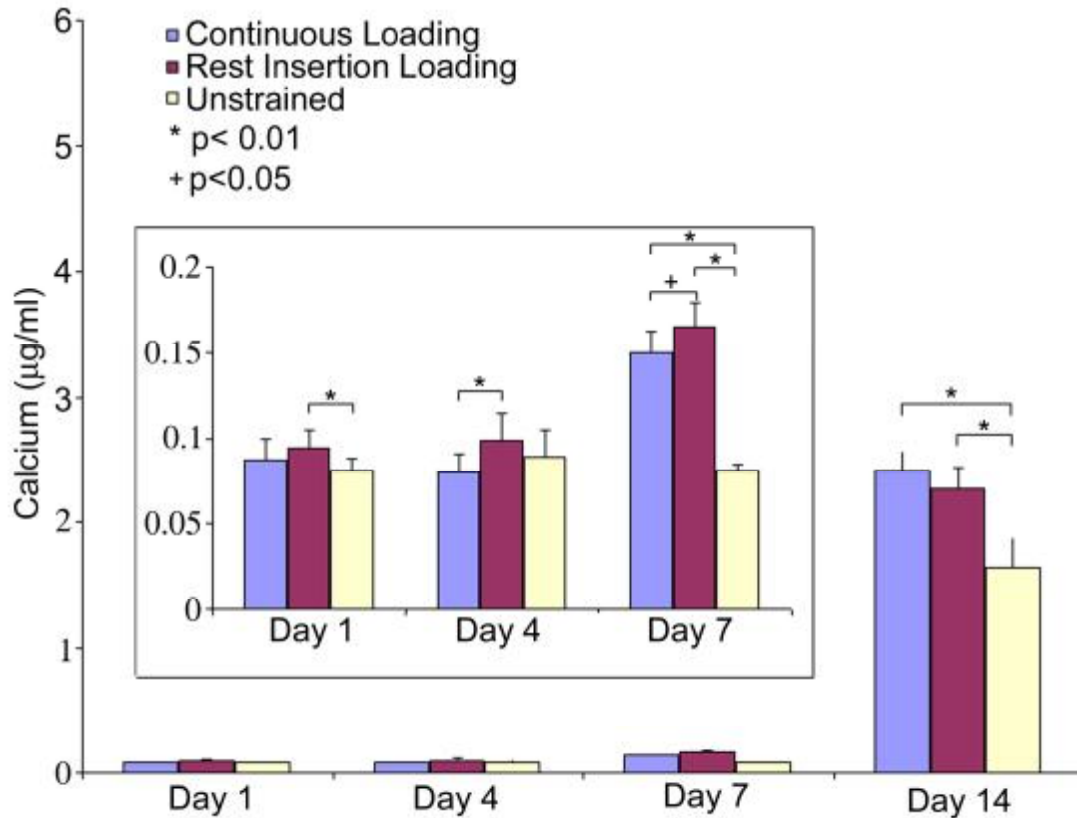


Figure 3. Calcium deposition of hADAS cells from donor 2 (low calcium deposition). Human ADAS cells cultured in osteogenic medium and exposed to one of the three loading conditions: continuous loading (10% strain, 1 Hz, 4 hrs), rest insertion loading (10% tensile strain, 1 Hz, 10 second rest insertion, 4 hrs), or unstrained.

Calcium deposition was very low in cells cultured in growth medium, regardless of loading regimen or cell line, and determined to be physiologically insignificant (data not shown).

3.2 Proliferation

Both hADAS cell lines, evaluated post confluency, exhibited similar trends in their proliferation. As measured by their metabolic activity, cells cultured in osteogenic medium, regardless of their loading condition, continued to proliferate throughout the entire two week study (Figure 4).

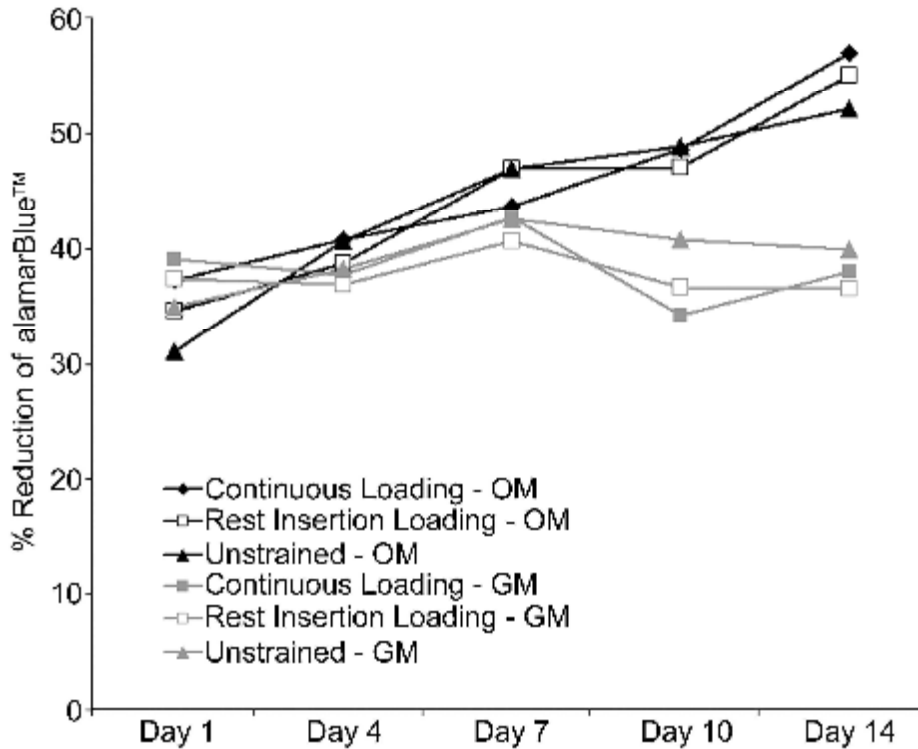


Figure 4. Proliferation of hADAS cells averaged from both donors when cultured in both osteogenic (OM) and growth medium (GM), measured as a percent reduction of alamarBlue™.

Continuously loaded cells showed an increase in percent reduction of alamarBlue™ from 37% to 57%, rest insertion loaded cells rose from 34.5% to 55%, and unstrained cells increased from 31% to 52%. Cells cultured in growth medium, however, did not show an increase in their percent reduction of alamarBlue™, signifying a stagnant growth over two weeks, regardless of loading conditions.

4. DISCUSSION

The use of adult mesenchymal stem cells for clinical applications in bone repair and/or replacement has gained significant attention in the past decade. However, the reproducibility and standardization of techniques has been hindered by evidence of donor variability. In this study, hADAS cell lines from two donors were selected and characterized for their ability to deposit calcium when cultured in osteogenic medium, specifically hADAS cells from one donor exhibited high calcium deposition and the other exhibited low calcium deposition. The donor variability shown in the present study is consistent with results by Phinney *et al.* who found expression of ALP, bone sialoprotein (BSP), and parathyroid hormone receptor (pTHR) mRNA expression varied widely among hMSCs from 5 donors, with 2 donors failing to express any significant induction of the three genes [131]. In contrast, 3 of the donors showed significant increases in ALP, BSP, or pTHR levels. Donors who were unable to express BSP, a calcium binding protein expressed by osteoblasts during bone repair, were also unable to deposit calcium after 22 days of continuous exposure to osteogenic medium. To our knowledge, the present study is the first to examine the effects of mechanical loading on hADAS cells with varying degrees of osteogenic potential.

It is well established in the literature that mechanical loading increases the osteogenic differentiation response of bone marrow-derived mesenchymal stem cells [52, 57, 111]. However, recent studies investigating the use of mechanical loading to induce osteogenesis have found that continuous loading causes mesenchymal precursor cells *in vivo* or osteoblasts *in vitro* to exhibit a phenomenon known as “diminishing returns” [119]. Observations that led those investigators to conclude two key mechanisms relevant to bone formation: 1) differentiation is not enhanced by longer loading regimens, and 2) mesenchymal precursor

cells do not need extensive loading to initiate differentiation. This nonlinear correlation between duration of loading and differentiation was described by Qin *et al.* [118] and Rubin *et al.* [15], each reporting a threshold for number of loading cycles when attempting to regulate bone mass in the ulnae of turkeys and roosters, respectively. Both studies found that a limit exists before mechanical loading failed to increase osteogenic response or, due to excessive loading, bone mineral content eventually decreased. Investigators have, therefore, implemented rest insertion loading in an attempt to restore mechanosensitivity in cells and therefore increase the osteogenic response to mechanical loading. In this study, we integrated a 10 second rest period between loading cycles to investigate any changes in osteogenic differentiation response of hADAS cell lines with either high or low calcium deposition capabilities.

Through quantification of calcium deposition, we found that both rest insertion and continuous cyclic tensile strain regimens increased osteogenic differentiation of hADAS cells compared to unstrained controls, consistent with what we know about the positive impacts of mechanical stimulation on osteogenic response of bone marrow-derived mesenchymal stem cells under mechanical stimulation. However, unlike what has been seen with MSCs, rest insertion loading did not cause ADAS cells to differ in their osteogenic potential as compared to continuous loading. This trend of increased mineral content in response to either continuous cyclic tensile strain or cyclic with rest insertion tensile strain was consistent for hADAS cells from both donors, although the high calcium depositing hADAS cell line responded better than the low calcium depositing cell line. These data suggest that hADAS cell lines that are more prone to produce bone will respond more favorably to mechanical stimuli as compared to cell lines that do not. Further analysis of the change in calcium

deposition from day 4 to day 7 reveal an increase of calcium deposition in mechanically strained samples from both hADAS cell lines, cultured in osteogenic medium, as compared to unchanged calcium levels in unstrained controls. These results may indicate that mechanical loading not only increases, but also accelerates, the osteogenic differentiation of hADAS cells.

Although the results of this study do not correlate with other rest insertion studies using bone marrow-derived MSCs, bone precursor cells, or osteoblasts with respect to increased osteogenic response with rest insertion, it is important to note that most of those studies were performed *in vivo* where other chemical stimulants may have been present or *in vitro* using different cell types. Further, and perhaps even more important, hADAS cells have been observed to respond differently than other mesenchymal cells in a multitude of ways including differentiation potential [41, 54], potential need for different medium supplements [81], or presenting different surface markers [47, 50]. This study provides further evidence that ADAS cells behave differently from MSCs and other cells in response to mechanical load by exhibiting an equally positive response to either continuous cyclic or cyclic with rest insertion tensile strain, with no immediately apparent beneficial osteogenic response to one paradigm over the other. However, ADAS cells are consistent with MSCs and other cell lines with respect to their positive osteogenic differentiation response to mechanical load.

Mechanical loading, either continuous or with rest insertion, did not seem to affect cell proliferation regardless of medium conditions. The proliferation assay used, alamarBlue™, reports an absorbance level that corresponds to cell metabolic activity and has been shown to be directly correlated to a specific number of cells [63, 135]. Using alamarBlue™, the measurements taken from post confluent cell cultures report the relative

number of cells but do not differentiate between cell types, whether they remain hADAS cells or mesenchymal precursor cells. Therefore, our results indicate that there was no change in metabolic activity between samples of all loading regimens, with a strong correlation that these samples, therefore, contained the same number of cells. It is also plausible to extrapolate that because there was no difference in proliferation, we can assume that under mechanical loading, more hADAS cells had undergone osteogenesis and were now osteogenic precursor cells. As a result of cyclic tensile strain, hADAS cells had accelerated and enhanced osteogenic differentiation resulting in a significant increase in mineralized extracellular matrix production.

In summary, this study revealed that while rest insertion loading did not increase the osteogenic effects of mechanical loading of ADAS cells over continuous cyclic tensile strain, mechanical loading, regardless of regimen, was able to increase the calcium deposition from hADAS cells compared to those that remained in static culture. Perhaps even more significant was the conclusion that mechanical loading improves osteogenesis of hADAS cells, in spite of initial osteogenic differentiation potential. However, high calcium-depositing hADAS cells respond more intensely to mechanical loading than cells that deposit low amounts of calcium. Not only did mechanical stimulation increase the magnitude of osteogenic differentiation of hADAS cells as measured by calcium deposition, but this study suggests that mechanical stimulation accelerates the rate of differentiation of hADAS cells compared to unstrained cells. These findings propose that ADAS cells may behave differently than other mesenchymal precursor cells *in vivo* and *in vitro*, but remain consistent in that mechanical stimulation is a potent stimulus for inducing ADAS cell osteogenic differentiation. This study not only validates the potential use of ADAS cells in tissue

engineered bone constructs, but also demonstrates the need for a better understanding of ADAS cell functionality.

SUMMARY

Mechanical loading can be a potent stimulator for osteogenic differentiation of bone-marrow derived mesenchymal stem cells (MSCs). However, continuous loading of MSCs can result in desensitization and eventual stagnant response to mechanical stimulation. To date, no studies have investigated the osteogenic response of adipose-derived adult stem (ADAS) cells to mechanical loads applied in either a continuous cyclic or cyclic with rest insertion loading approach. The purpose of the previous study was to investigate the effects of continuous cyclic tensile strain and cyclic with rest insertion tensile strain on osteogenic differentiation of human ADAS (hADAS) cells; and, the influence of these mechanical loads on two hADAS cell lines with distinctly disparate osteogenic differentiation capabilities (i.e. hADAS cells that exhibit either high calcium deposition in osteogenic differentiation medium or low calcium deposition in osteogenic differentiation medium). Results showed that both continuous cyclic tensile strain and cyclic with rest insertion tensile produced a significant increase in calcium deposition for both high and low calcium depositing hADAS cell lines as compared to unstrained controls. There was no difference in this positive response for either continuous cyclic or cyclic with rest insertion tensile strain. Results further showed that cyclic tensile strain, both with and without rest insertion, increased the rate of differentiation induction. However, mechanical stimulation had a much stronger effect on the high calcium depositing hADAS cell line than on the low calcium depositing hADAS cell line, suggesting that mechanical loading has a greater effect on cell lines that already have an innate ability to produce bone compared to cell lines that do not.

CHAPTER 3: LITERATURE REVIEW – SCAFFOLDS FOR BONE TISSUE ENGINEERING

1. GRAFTS FOR CRITICAL SIZE BONE DEFECTS

At present, autografts and allografts are considered the gold standard for bone grafting. Autografts are osteoinductive, osteoconductive, and have osteogenic properties [136]. However, they have also been associated with donor site morbidity [83, 137, 138], chronic pain, nerve damage, infection, fracture, pelvic instability, hematoma, and tumor transplantation [139]. Allografts negate these concerns but have their own limitations. Allografts carry the risk of causing an immune response in the host, transferring diseases to the host [140] and/or weakening the allograft's biological and mechanical properties that would have made it an ideal replacement for bone constructs during the storage and transplant process [141].

The limitations of autografts and allografts have led to the development of natural and synthetic polymers for bone grafts. Scaffolds are a key component for developing a tissue engineered bone construct for implantation into a critical bone defect. Ideally, a scaffold should contain the following characteristics for successful implantation: 1) be biocompatible and bioresorbable with a controlled degradation rate to match cell/tissue growth *in vivo*; 2) have mechanical properties capable of withstanding the mechanical loads experienced in the physiological environment during cell matrix maturation; 3) be three-dimensional and allow for adequate diffusion for cell growth, nutrient delivery, and waste removal; and, 4) have suitable surface chemistry for cell attachment, proliferation, and differentiation [142]. Several materials, fabrication techniques, and modifications have been implemented over the years to achieve these characteristics for use in clinical applications.

2. ARCHITECTURE OF SCAFFOLDS

The success of bone formation relies heavily on the pore size and porosity of the scaffold [143, 144]. Native trabecular bone has a porous environment with a porosity >75% [145] and typical pore sizes approximately 1 mm in diameter [146]. In addition, cells that are more than 200 μm from a blood supply have reduced viability due to low oxygen supply [147]. Klenke *et al.* has recently shown that there is a direct relationship between pore size, vascularization, and bone formation [148]. They found that scaffolds containing pores $\geq 140 \mu\text{m}$ had significantly higher vascular ingrowth and bone formation compared to scaffolds with smaller pores. Their results were consistent with Robinson *et al.* who that demonstrated a relationship between increasing pore size and bone ingrowth, with optimal pore sizes for bone formation $\leq 350 \mu\text{m}$ [144].

Porosity has also been shown to be important for cell proliferation, as evidenced by Takahashi *et al.* who reported higher proliferation of MSCs on polyethylene terephthalate fabrics with higher porosities compared to those of lower porosities [149]. The increase in cell proliferation was attributed to the larger area for cells to migrate and an increase in oxygen and nutrient supply. Although larger pore sizes and porosities are beneficial for vascularization and bone formation, they can also lead to decreased compressive strength [150, 151].

3. FABRICATION TECHNIQUES

Natural and synthetic scaffolds can be fabricated using several methods, such as electrospinning, fiber bonding, solvent casting and particle leaching, or non-woven techniques, among others [152]. Electrospinning involves preparing the polymer solution and

placing it into a syringe. The polymer is drawn from the syringe by a combined force of gravity and electrostatic charge provided by a high voltage power supply. The positively charged polymer stream is collected on a negatively charged collector plate, placed at a designated distance away from the syringe. The polymer viscosity, speed of polymer extrusion, voltage, and plate distance controls the pore size and porosity of the resulting scaffold.

Solvent casting and particle leaching involves dispersing mineral or organic particles into a polymer solution [152]. The particles are eventually leached out using appropriate dissolutions, creating a porous polymer matrix. Using this method, matrices can be fabricated with up to 93% porosity and mean pore size of 500 μm . The limitation of this process, however, is that only thin wafers or membranes up to 3 mm thick can be manufactured. Therefore, large three-dimensional scaffolds necessary for bone constructs to fill critical sized defects would not be easily produced.

Melt-blowing, a non-woven technique, involves similar steps as electrospinning where a polymer of low viscosity is extruded from a syringe at high speed and collected on a moving or rotating plate [153]. As the polymer is extruded from the syringe, it is subjected to two hot air streams to form the fiber [132]. Similar to electrospinning, pore size and porosity can be modified by varying the polymer viscosity, speed of extrusion, plate distance and temperature gradient of the polymer melt. These fibers are typically 1-5 μm in diameter and can be modified via the same variables.

4. SCAFFOLD MATERIALS FOR TISSUE ENGINEERED BONE CONSTRUCTS

Natural Materials

Natural polymers for tissue engineering provide favorable properties for *in vivo* implantation due to their more common characteristics of being non-toxic, biocompatible, osteoinductive, and/or osteoconductive [154]. Some of the most popular natural polymers used in tissue engineering of bone are collagen [155, 156], chitosan [157-159], hydroxyapatite [160, 161], and demineralized bone [162, 163]. Collagen, the most abundant protein in the body, has been extensively investigated for biomedical applications. Collagen is a biocompatible, biodegradable, osteoinductive material [164, 165]. In addition, it has properties, such as surface proteins, that make it an ideal material for cell attachment, proliferation, and differentiation [166]. For example, Kakudo *et al.* was successful in using a three-dimensional (3D) hADAS seeded collagen scaffold for a bone construct. After being cultured *in vitro* for 14 days, these scaffolds were able to induce cell ingrowth and osteogenic differentiation with the addition of osteogenic supplements in the culture media [155]. Once grown *in vitro*, these scaffolds were implanted into nude mice and new bone formation occurred. In another application, Shih *et al.* showed that osteogenic differentiation of bone marrow-derived hMSCs was significantly higher for cells grown on type I collagen nanofibers compared to those seeded on polystyrene tissue culture plates [156].

Although these studies concluded that collagen is a suitable material for tissue engineered bone scaffolds, collagen alone typically does not provide the mechanical strength needed for an effective bone replacement. For this reason, collagen has been modified from its original form by combining it with other materials. Collagen-hydroxyapatite composites have been investigated in order to produce a more biocompatible, biodegradable,

osteoinductive material, while also maintaining rigidity and mechanical stability [167-172]. Rodrigues *et al.* used this combination of materials to create a human osteoblast-seeded scaffold for bone engineering applications [170]. They observed that osteoblasts exhibited a high degree of proliferation and were securely attached to the surface. In addition, cells migrated through the composite and began covering the surface of the material 11 days post seeding [170]. In order to test the enhanced mechanical properties of a porous collagen/hydroxyapatite composite, Yunoki *et al.* showed that during compression tests at 30% strain, the shape of the specimens were well recovered [167]. They also reported that the composite was able to withstand higher compressive stress, attributed to the reinforcement of hydroxyapatite nanocrystals in the collagen matrix, than other porous materials with biopolymers.

Demineralized bone matrix is another widely used natural scaffold material. Demineralized bone matrices are created by obtaining bone from a subject (either from patient or another donor), desolving the mineral, and then partially defatting it [163]. Once the matrix is prepared, the demineralized bone matrix is seeded with MSCs or osteoblasts. Demineralized bone is thought to contain properties that cause MSCs to differentiate. Urist *et al.* proposed that a low molecular weight oligosaccharide glycoprotein exists in the intercellular matrix and perilacunar walls that is exposed when bone is demineralized and this glycoprotein causes differentiation when it comes into contact with surrounding cells [173]. Einhorn *et al.* tested this hypothesis by implanting a demineralized bone matrix, obtained from male Sprague-Dawley rats, into a fracture site. After 12 weeks post implantation, five of the seven animals treated with a demineralized bone matrix were found to have a bridging callus and union across the fracture [163]. In contrast, those animals not

treated with demineralized bone matrices demonstrated non-union, were grossly unstable, and were unable to undergo mechanical testing. When limbs of animals treated with demineralized bone matrices were mechanically tested, they showed improved resistance to fracture and increased strength, values comparable to early fracture repair, as compared to animals treated only with pins. The success of this type of bone replacement has led to commercially available demineralized bone matrices such as Allomatrix, demineralized bone matrix plus sodium hyaluronate (DBX), DBX with poly(DL-lactide) mesh, Dynagraft, Grafton, and Regenafil [162]. One main concern with these commercial products, however, is the lack of regulation by the FDA. Therefore, methods of sterilization vary, in turn creating products with unreliable properties that may make the implant inferior or invoke an immune response [174].

Synthetic Polymers

Although there are many separate and distinct advantages to several of the natural polymers described above, one natural material alone does not contain all of the required components for a successful bone replacement. Synthetic polymers provide an abundant source of material that can be used in bone grafts and can be easily fabricated and modified to fit the mechanical, structural, and chemical properties required for the specific application. Of the polymer blends available, the more commonly used are poly(lactic acid) (PLA), poly(glycolic acid) (PGA), and their copolymer poly(lactic-*co*-glycolic acid) (PLGA) [175, 176]. These materials are attractive because of their biocompatibility [175-177], degradation rates [178], and osteoinduction properties [176]; they are FDA approved and have been in use for over 20 years.

The family of PLA is by far the most commonly used synthetic biomaterial [152]. PLA exists as either poly(L-lactic acid) (PLLA) or poly(D,L-lactic acid) (PDLLA), but PLLA is the most common form found in tissue engineering applications. Poly(L-lactic acid) is widely used as a scaffold material for bone constructs because of its degradation properties [142, 178], biocompatibility [179], and material properties that can be easily modified by changes in molecular weight [178, 180, 181]. Polylactic acids are semi-crystalline and relatively hard materials with a glass transition temperature of 65°C and melting temperature of between 170-180°C [152]. Specifically, PLLA's crystallinity is reported to be approximately 65% and can be melt-processed at 200-250°C, depending on the molecular weight. The degradation of PLLA *in vivo* is relatively slow compared to PGA, which is more hydrophilic and tends to be completely absorbed by 4 weeks post implantation [152]. Although PGA is more cell friendly, its fast degradation limits its use in bone constructs [180]. To counter PGA's relatively fast degradation rate, Moran *et al.* used PLA to reinforce a PGA scaffold using for cartilage tissue engineering by coating it with either 0, 12, 27, 52, or 68% PLA by mass fraction [180]. The degradation of the composite scaffold increased as the PLA content was increased, ranging from 5-45 days. In addition, the modulus of elasticity was increased according to increased amounts of PLA, with a > 20-fold increase in modulus from a scaffold with 68% PLA compared to PGA alone. To evaluate the material properties of porous PLLA foams, Lu *et al.* measured the compressive strains of foams with three different porosities (70-90%) (molecular weight approximately = 130000 Daltons) during the degradation process [178]. The molecular weight of all foams decreased exponentially with degradation time. Correspondingly, the strain after 60 minutes of compressive loading (9.5 kPa) was approximately 0.15 for all foams prior to degradation, and

decreased to below 0.07 after 46 weeks of degradation. The porous nature of the PLLA foams, as well as the decrease in molecular weight during degradation, is attributed to the faster degradation and decrease of mechanical properties.

Unfortunately, biological reactivity with PLLA is very poor and this limits its functionality as a scaffold material unless modified. The preference for cells to adhere on a modified PLLA structure compared to PLLA alone has been well documented [175, 182-186]. Chu *et al.* reported an increase in adhesion of human endothelial cells to ammonia plasma modified PLLA and fibronectin-coated modified PLLA substrates compared to PLLA controls or fibronectin-coated PLLA controls [182]. Likewise, Jiao *et al.* found that osteoblast-like cells adhered to and proliferated better on PLLA scaffolds modified with chitosan compared to PLLA alone [175]. Further evaluation revealed that cell attachment efficiency also increased on hybrid scaffolds compared to PLLA alone, a phenomenon suggested to be the result of three factors: 1) increasing the hydrophilicity of the substrate with the incorporation of chitosan, which favors cell compatibility; 2) chitosan has a similar structure to glycosaminoglycan, providing more desirable sites for cell adhesion; and, 3) additional micropores were created during the fabrication of the hybrid scaffold, increasing the surface area to volume ratio.

Mechanical Properties

A major component to the success of a scaffold for bone replacement is that it withstands the physiological loads *in vivo* until native extracellular matrix develops. Trabecular bone is reported to have a compressive strength of 4-12 MPa and a modulus of 0.02-0.5 GPa [152]. In order to match these values, researchers have found that by modifying

the molecular weight of polymers, different mechanical properties can be achieved [187]. However, these mechanical properties will shift as the polymer degrades in the body and therefore the degradation and resorption kinetics of the polymer must be well understood. For a successful repair, the bioresorbable scaffold must retain its physical properties for at least 6 months (4 months *in vitro* during cell culture and 2 months *in vivo*) [142]. The strength and stiffness of the scaffold should match that of the host tissue until new tissue has replaced the degrading scaffold matrix.

Modification of PLLA

The results of the studies described above reveal how modifying the surface of PLLA through chemical or morphological methods can enhance cell-substrate compatibility. Some of the methods used to modify scaffold substrates include material composition [183, 188, 189], surface topography [185, 190, 191], and surface chemistry [184, 185, 190, 192-194]. Surface chemistry of biomaterials plays a critical role in cell adhesion and growth.

Poly lactide polymers exhibit hydrophobic properties because they do not contain a function group in their side chains, such as a carboxyl group (COOH) or a hydroxyl group (OH) [184, 195-198]. This is not an ideal environment for cells, which are more likely to bind to hydrophilic surfaces [182, 184, 185].

Plasma treatment is one method to increase hydrophilicity by adding functional groups to the surface of materials [190, 195, 197, 198]. With the addition of functional groups, cells present a more favorable response in terms of cell adhesion, proliferation, and morphology [182, 184, 185, 190, 196-198]. In particular, numerous studies have investigated the cellular response to plasma treatment of PLLA. Nakagawa *et al.* seeded MC3T3-E1 cells

onto atmospheric, carbon dioxide (CO₂), or perfluoro propane plasma treated PLLA and found that cell response was better on substrates treated with air or CO₂ plasma [184]. Cell adhesion and proliferation was increased for MC3T3-E1 cells seeded on either of these substrates. Yamaguchi *et al.* had similar responses when Chinese hamster ovary cells were seeded on PLLA which was oxygen plasma treated [185]. Not only did these cells exhibit accelerated adhesion on plasma treated PLLA compared to PLLA alone, but cells seeded on plasma treated PLLA proliferated in sheets resembling biological tissue compared to the balled up and separated structure of cells adherent to controls.

**CHAPTER 4. THE EFFECTS OF OXYGEN PLASMA TREATMENT ON HUMAN
ADIPOSE-DERIVED ADULT STEM CELL ADHERENCE TO POLY(L-LACTIC
ACID) SCAFFOLDS**

A.D. Hanson, M.E. Wall, B. Pourdeyhimi, and E.G. Lobo

The following chapter investigates the response of hADAS cell adhesion to oxygen plasma treated nonwoven PLLA scaffolds. We are interested in determining the relationship between the increased hydrophilicity of porous PLLA and cell adhesion characteristics.

1. INTRODUCTION

Tissue engineered load-bearing constructs include cell-seeded scaffolds for future implantation *in vivo* [40, 46, 73, 98, 199-201]. In some cases, enhanced cellular adhesion has controlled whether cells proliferate and differentiate [185, 186]. However, the polymers used in tissue engineering applications are selected for their biocompatibility and mechanical properties [142, 202, 203], and, thus, they may not provide the best surface environment for cell attachment.

Poly (L-lactic acid) (PLLA), which is both biocompatible and bioabsorbable [179], has been found to exhibit a more optimal environment for cellular adhesion as compared to poly ϵ -caprolactone and poly(lactic-co-glycolic acid) [188]. In general, however, PLLA exhibits poor cell-surface adhesion properties due to its hydrophobic nature [203-205]. Polylactide polymers do not contain functional groups, such as a carboxyl group (COOH) or a hydroxyl group (OH), which enhance cell adhesion by increasing surface hydrophilicity [184, 195-198]. Scaffold material composition [115, 183, 188], surface chemistry [184, 185, 190, 192-194], and surface topography [185, 190, 191] can all affect cell adhesion. Plasma treatment has been used to add functional groups to polymers, thus altering surface chemistry and topography [184, 185, 190, 192, 194, 198] and increasing hydrophilicity [184, 185, 190, 198]. In turn, cells more readily adhered to these plasma treated surfaces [184, 185, 195], increased their strength of adherence [190, 192], and altered their morphology [185]. Oxygen plasma, in particular, has been successfully used to add hydroxyl groups to the surface of various polymers and, thus, improve cell attachment [185, 190]. Protein adsorption to polymers [206, 207] and coating substrates with extracellular matrix proteins such as

fibronectin, laminin, collagen, or vitronectin [186, 208, 209] are some other substrate treatments which have been used to enhance cell affinity for polymers.

Besides the need for suitable polymers that provide adequate cellular adherence, the other major component of tissue engineered constructs is cells. Adipose-derived adult stem cells have gained increasing interest for musculoskeletal tissue engineering over bone marrow-derived hMSCs because of the relative abundance of excess adipose tissue and the large number of cells that can be isolated from the tissue. Additionally, hADAS cells have similar differentiation ability as bone marrow-derived hMSCs [41, 47, 210-213].

Studies have found that human bone marrow-derived MSCs can adhere to PLLA [62, 214, 215]. However, there are no studies that have analyzed whether oxygen plasma treatment of PLLA affects hADAS cell adhesion. Advances in polymer manufacturing have allowed for the creation of melt-blown polymers with defined pore sizes and porosities using a variety of biocompatible polymers. Given these capabilities, this study investigates the potential use of a non-woven, melt-blown scaffold for tissue engineering; in particular, for the analyses of hADAS cell adhesion, proliferation and eventual differentiation within a plasma-treated, melt-blown, non-woven PLLA scaffold. The aim of this study was to evaluate the effects of oxygen plasma treatment on cell morphology, viability, and adhesion rates of hADAS cells seeded on non-woven PLLA scaffolds. It was hypothesized that plasma treatment would increase the number of hADAS cells that adhered to a melt-blown, non-woven PLLA scaffold without affecting cell viability.

2. MATERIALS AND METHODS

2.1 Manufacturing of PLLA Scaffolds

Scaffolds for this study were produced at the Nonwovens Cooperative Research Center at North Carolina State University (Raleigh, NC, USA). Scaffolds were produced using a melt-blowing process.

The melt-blowing process was first introduced by Wentz [216] as a means to create a collection medium for radioactive particles in the upper atmosphere. The melt-blowing, non-woven process is a unique technology in which molten polymer emerging from a series of small orifices on the die is subjected to two hot, high velocity air streams that cause attenuation and fibrillation of the polymer into very fine fibers. The fibers made in this process are typically 1-5 μm in diameter. Owing to their small fiber diameter and high surface area, melt-blowing substrates are typically used as barrier layers and filters. During melt blowing, the fibers are deposited on a moving collector belt, usually creating a layer of self-bonded fibers. The basis weight of a melt-blown fibrous layer can be varied by adjusting the speed of the collector belt. The die cross-section is shown in Figure 1. The melt-blowing process requires polymeric melts to be of a very low viscosity, which is usually achieved by using a polymer with a high melt-flow rate and by adjusting the melt temperature during processing. Once the fiber breaks loose from the molten polymer pool at the die tip, it is propelled downward to the collector belt. The die to collector distance (DCD) and the air jet velocity determine the amount of time a newly created fiber spends suspended in air before it is forced into contact with the rest of the fibrous substrate during collection process. The melt temperature, air velocity, air temperature, and DCD have major influences on how much

solidification and crystallization occurs before the fiber comes in contact with other fibers already on the collector belt.

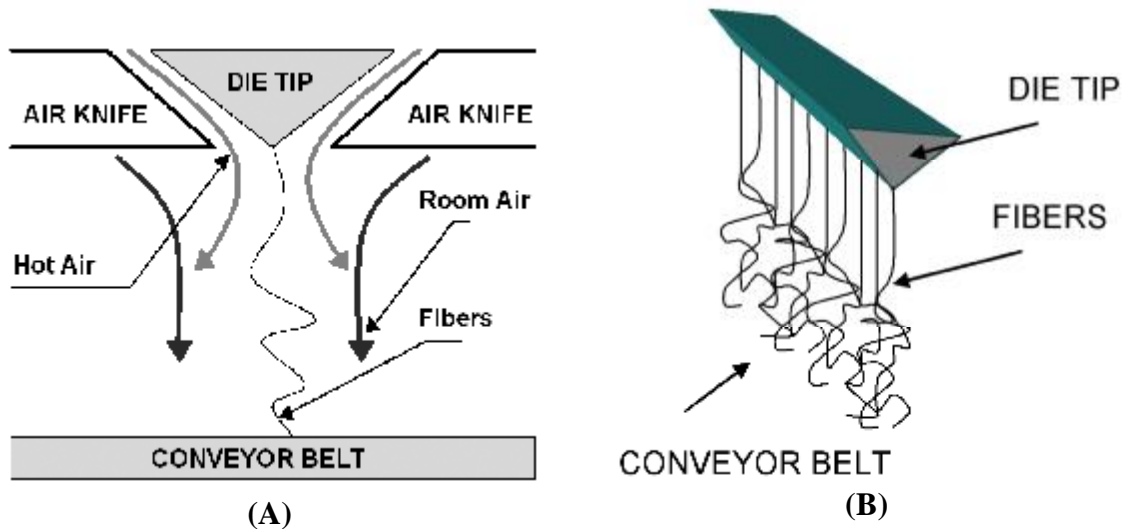


Figure 1. (A) Cross-section of fiber attenuation in the melt-blown process. Fibers are drawn attenuated by hot air. (B) Fibers are drawn, touch one another and self-bond before being collected on the conveyor belt.

Overall, filaments produced by the melt blowing process have generally low molecular orientation [217]. Fibers are typically between 1 to 5 μm . By lowering the throughput, fibers as small as 0.5 – 1 μm diameter can be formed.

2.2 Determination of Pore Size and Porosity

A SEM image of the melt-blown, non-woven PLLA scaffold is shown in Figure 2. Pore size was analyzed by using image analysis software which allows for the calculation of pores based on the measurement and conversion of area of pixels converted to real units of μ^2 . The procedure has been described previously [218, 219]. In melt-blown structures, the pore size typically is normal (some are lognormal). Thus, we report the average pore size

and the spread of the distribution. The average pore size was calculated to be approx. 1950 μm^2 with a range of 40 - 71840 μm^2 .

The porosity of the scaffold was determined by using the following equation [220]:

$$\Phi = 1 - \frac{\rho_s}{\rho_{\text{PLLA}}}$$

where Φ is porosity, ρ_s is the apparent density of the scaffold and ρ_{PLLA} is the true density of PLLA (1.25 g/cm^3). The apparent density was calculated and averaged by measuring the area of the scaffold and the thickness ($n = 3$). The porosity of the PLLA scaffold was found to be approx. 96.8%.

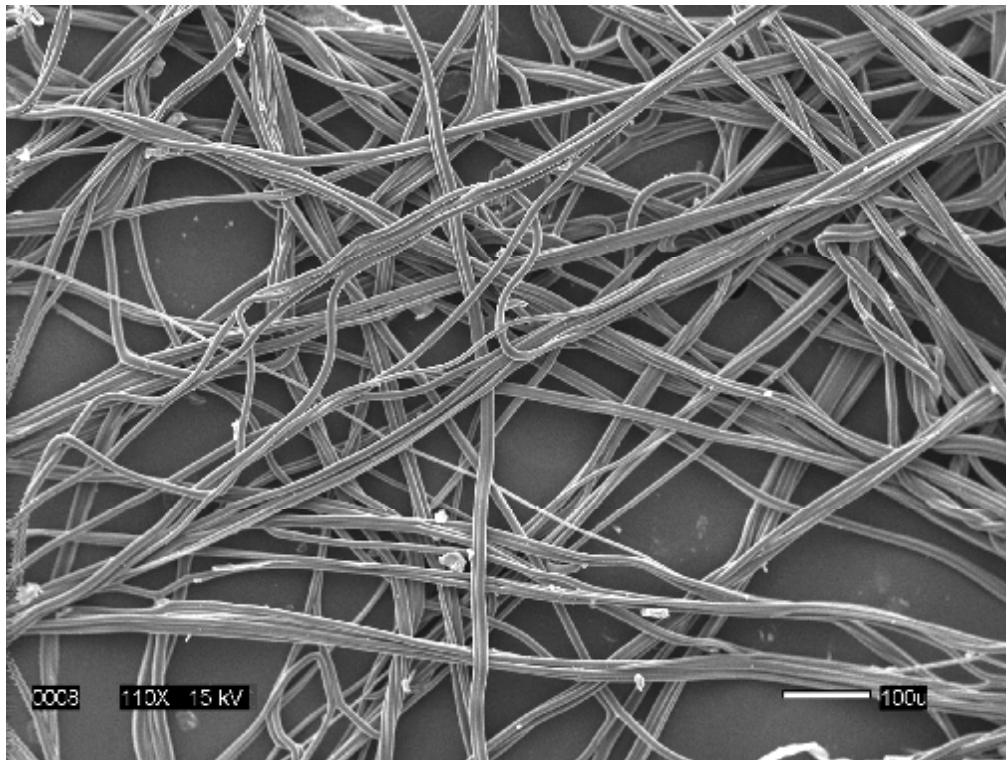


Figure 2. SEM picture depicting morphology of non-woven PLLA scaffolds; note the openness of the structure and the large fiber diameters formed by PLLA. This is partly due to the high viscosity of the polymer. Smaller fiber diameters are possible if the viscosity of the polymer is reduced.

2.3 Oxygen Plasma Treatment of Scaffolds

Scaffolds were soaked in 70% ethanol for 10 min and subsequently washed with de-ionized water for 10 min prior to treatment. Oxygen plasma treatment of the PLLA was performed using a Plasma Enhanced Chemical Vapor Deposition System (Premitec, Raleigh, NC, USA). A three-dimensional non-woven PLLA scaffold was placed in the vacuum chamber and internal pressure was lowered to 200 mTorr. Oxygen gas was introduced into the chamber at a power of 100 W for 10 min [190]. The vacuum chamber internal pressure was then returned to 760 Torr, and the PLLA scaffold was removed.

2.4 Measurement of Hydrophilicity for PLLA Scaffolds

Three PLLA films were made using a hot press to flatten PLLA pellets. A goniometer (Rame-Hart, Mountain Lakes, NJ, USA) was used to measure the hydrophilicity of these films. Static water droplets, 2 μ l each, were used to measure the contact angles of the PLLA films before and after oxygen plasma treatment.

2.5 Cell Isolation and Culture

Human ADAS cells were isolated from excess adipose tissue remaining from abdominoplasty or liposuction procedures conducted at UNC Hospitals in accordance with an approved IRB protocol. Tissue samples were obtained from three female donors (24-31 years old) of either Native American or Caucasian descent. Human MSCs were isolated from the adipose tissue and characterized as previously described by our lab [51]. Cells were seeded into T-75 culture flasks and maintained in complete growth medium (minimum

essential medium eagle, alpha-modified supplemented with 10% FBS (Atlanta Biologicals, Lawrenceville, GA, USA), 2 mM L-glutamine, 100 units/ml penicillin, and 100 µg/ml streptomycin). Once hADAS cells reached 70% confluency, cultures were washed twice with PBS and cells were removed from flasks with 0.05% trypsin/0.53 mM EDTA. All cell culture chemicals and supplies were purchased from Mediatech, (Herndon, VA, USA) and GIBCO BRL (Grand Island, NY, USA) unless otherwise noted.

2.6 Seeding of Cells into Scaffolds

Human ADAS cells at passages three and four were grown in T-75 culture flasks until reaching 70% confluency, at which point cells were trypsinized and seeded onto 36 plasma-treated PLLA scaffolds or 36 untreated scaffolds at a cell seeding density of $(60-90) \times 10^3$ cells/ 200 µl of complete growth medium in a 96-well plate. Cells were analyzed for cell adherence, morphology, and viability beginning 2 hours post-seeding.

2.7 Visualization of Cell Morphology

At 2, 4, 8, 12, and 24 hours after cell seeding, scaffolds were removed from the 96-well plate, washed twice with PBS and fixed with 10% formalin for 15 min. Cells were then stained with Harris-modified hematoxylin with acetic acid (Fisher Scientific, Hampton, NH, USA) for 8 minutes and again washed with PBS until residual stain was removed from the scaffold material. Scaffolds were mounted in wells made from polydimethylsiloxane on glass slides and viewed using a fixed stage microscope at 20× magnification. In order to assess cell morphology, images of the scaffold were visually analyzed by two observers and scored based on the percent area of each image with adherent cells (number of cells) and the

percentage of these adherent cells that had begun to spread out and the degree to which they were spread (cell spreading). Evaluation of the degree of cell spreading was based on how well cells elongated along and spread between the fibers and how much of the pores were filled in by the cells. The following percent scale to score the images: 0-10% (+/-), 10-30% (+), 30-60% (++), and 60-100% (+++).

2.8 Cell Viability Assay

Cell viability was assessed at 2, 4, 8, 12, 24, and 48 hours after seeding. Scaffolds were washed twice with PBS and stained for 10 min with 4 μ M calcein AM to label live cells and 4 μ M ethidium homodimer-1 to label dead cells (Molecular Probes, Eugene, OR, USA). Scaffolds were then mounted onto slides and viewed under a fluorescence microscope at 10 \times magnification. Cell viability was evaluated by visual inspection.

2.9 Adhesion Quantification

The number of hADAS cells that adhered to the PLLA scaffolds was determined by extracting DNA from cells within the scaffolds. At 2, 4, 8, 12, 24, and 48 h after seeding, cells were lysed using a freeze-thaw method, followed by crushing of the scaffolds using a pestle, and finally sonicating the samples to remove any residual DNA. DNA was labeled with Hoechst 33258 (Molecular Probes, Carlsbad, CA, USA), and the fluorescent signal was analyzed with a microplate reader (Tecan, Durham, NC, USA). The signal was standardized to known DNA amounts representative of known cell numbers. Student's t-tests were used to determine significant differences ($P < 0.05$) in cell adherence between the two conditions.

3. RESULTS

3.1 Hydrophilicity of PLLA after Plasma Treatment

Three PLLA films were created to measure the change in contact angles after oxygen plasma treatment. The contact angle, associated with the level of PLLA hydrophilicity, decreased from an average of $75.6^{\circ} (\pm 3.47)$ to $58.2^{\circ} (\pm 3.42)$ ($p < 0.05$) when films were oxygen plasma treated, indicating that the PLLA films became more hydrophilic.

3.2 Cell Morphology and Distribution

In general, hADAS cells from all three donors had a greater distribution throughout the scaffolds and were more spread-out and elongated along fibers and within the pores of scaffolds that were plasma treated (Table 1). At 2 hours, cells seeded on untreated scaffolds formed clusters around individual fibers and remained rounded (Fig. 3A). Additionally, the untreated scaffolds had areas of sparse cell attachment and regions with larger clusters of cells (Fig. 4A). In contrast, cells seeded on plasma treated scaffolds had begun to spread along and across the fibers (Fig. 3B) and were more evenly distributed throughout the entire scaffold (Fig. 4B). As scaffolds continued to incubate, cell spreading (Fig. 3) and distribution throughout the scaffold (Fig. 4) increased on both treated and untreated scaffolds. However, even 4 hours after seeding, cells on plasma treated scaffolds continued to exhibit more pronounced cell spreading and uniform cell distribution throughout the scaffold as compared to the untreated controls (Fig. 3C and 3D). Plasma treated scaffolds still had a more even distribution of hMSCs compared to the untreated scaffolds at 12 hours (Fig. 4C, 4D). By 24 hours, there was no difference between cell distribution (Fig. 4E and 4F) or spreading (Fig. 3E, 3F) of cells seeded on plasma treated or untreated scaffolds.

Table 1. Effects of oxygen plasma treatment on cell adherence and spreading within melt-blown, non-woven PLLA scaffolds. (“+/-” = 0-10%; “+” = 10-30%; “++” = 30-60%; “+++” = 60-100%)

Time post-seeding (hours)	Scaffold condition	Number of cells	Cell spreading
2	Untreated	+	+/-
	Plasma treated	++	+
4	Untreated	+	+
	Plasma treated	++	++
8	Untreated	+	++
	Plasma treated	++	+++
12	Untreated	+	++
	Plasma treated	++	++
24	Untreated	+++	+++
	Plasma treated	+++	+++

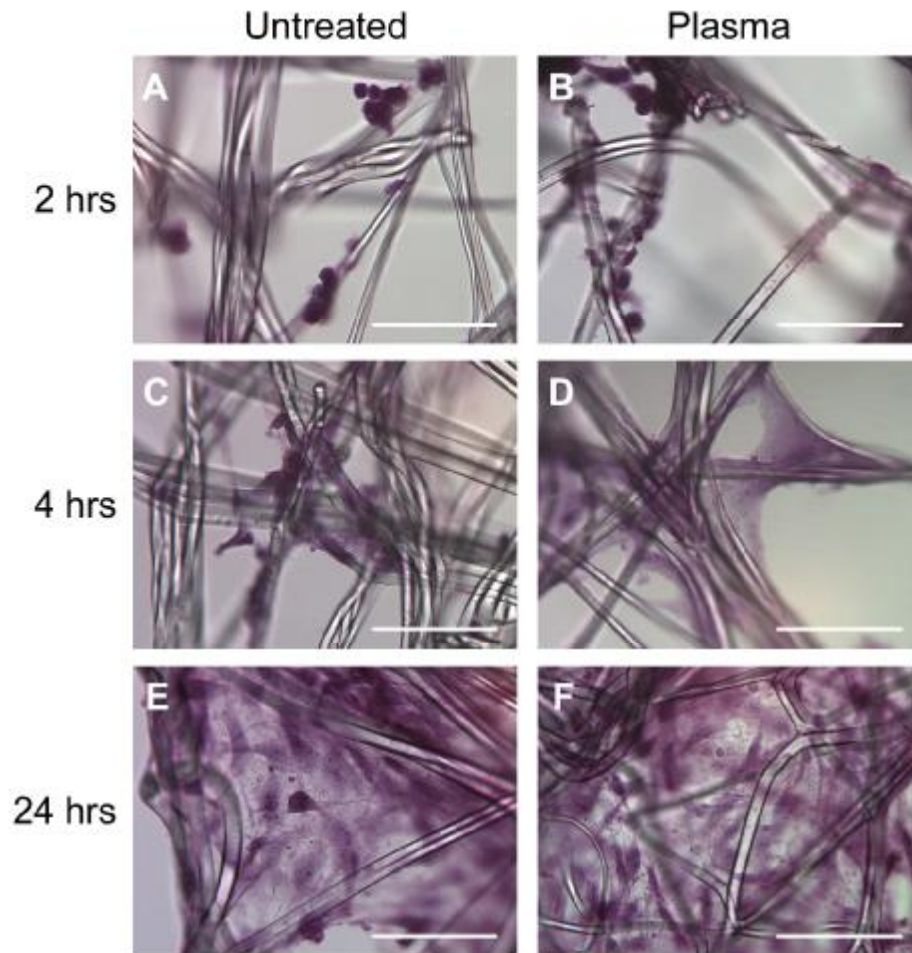


Figure 3. Effects of oxygen plasma treatment of PLLA scaffolds on cell spreading. Representative images of hematoxylin-stained adipose-derived adult stem cells depicting cellular morphology on untreated (A, C, E) or oxygen plasma treated (B, D, F) melt-blown, non-woven PLLA scaffolds at 2 (A, B), 4 (C, D), and 24 (E, F) hours after cell seeding. Scale bar = 20 μm .

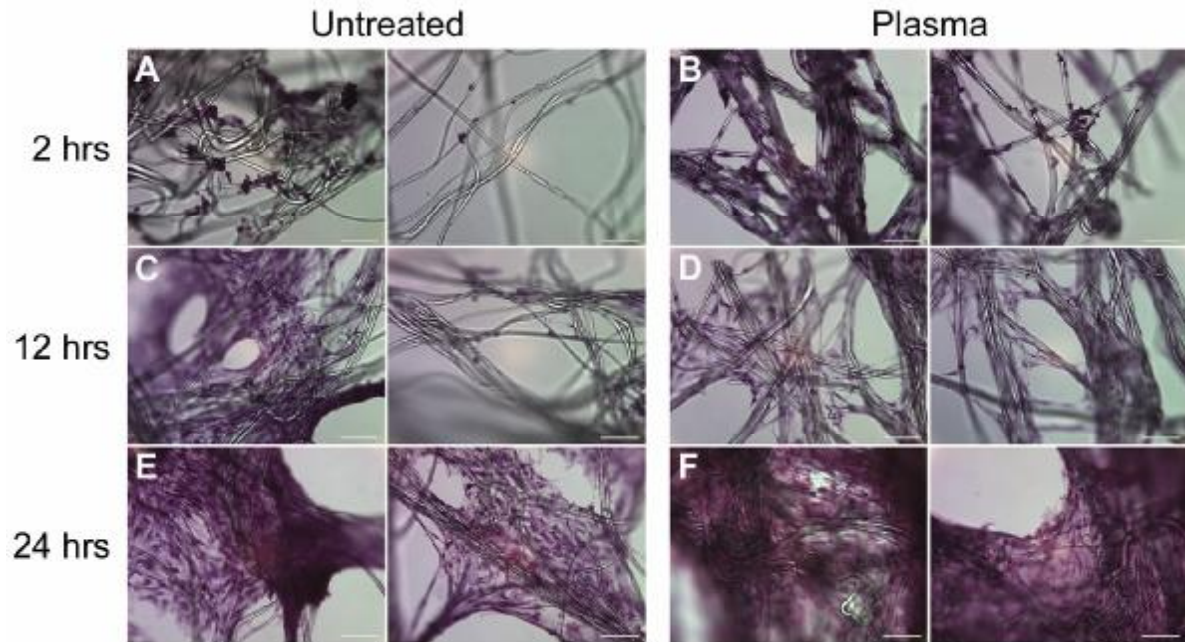


Figure 4. Effects of oxygen plasma treatment of melt-blown, non-woven PLLA scaffolds on the distribution of human adipose-derived adult stem cells throughout the construct. Representative images of hematoxylin-stained cells within two representative areas of an untreated (A, C, E) or an oxygen plasma treated (B, D, F) scaffold at 2 (A, B), 12 (C, D), and 24 (E, F) hour post-seeding. Scale bar = 20 μ m.

3.3 Cell Viability

Visual assessment of fluorescently stained hADAS cells revealed no difference in viability between cells seeded on plasma-treated and untreated scaffolds. Cells on both scaffolds remained viable throughout the 48 hour time point, with no change from 2 to 48 hours after initial seeding (Fig. 5).

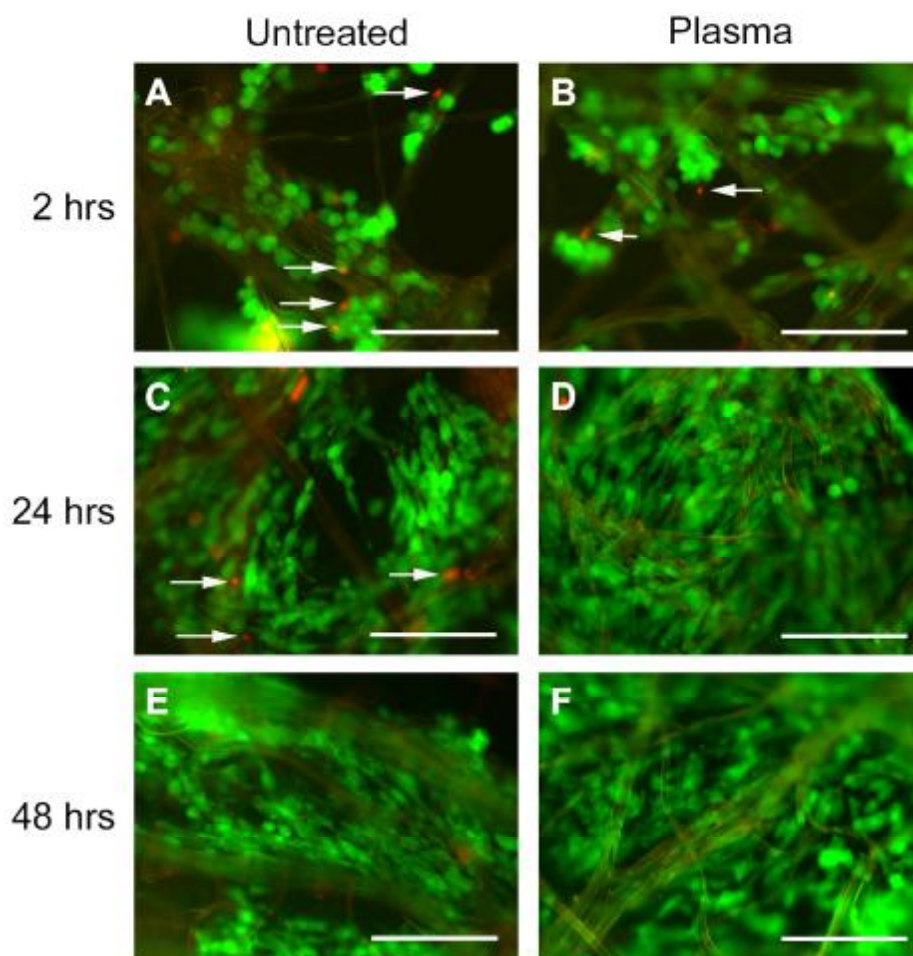


Figure 5. Effects of oxygen plasma treatment of PLLA scaffolds on cell viability. Representative images of human adipose-derived adult stem cells seeded on untreated (A, C, E) and oxygen plasma treated (B, D, F) PLLA scaffolds stained with calcein AM (green) and ethidium homodimer-1 (red, arrows) to label live and dead cells, respectively, at 2 (A, B), 24 (C, D), and 48 (E, F) hours post-seeding. Scale bar = 10 μ m.

3.4 Adhesion Quantification

Each donor was analyzed individually, due to patient-to-patient variability, to determine if there was a significant difference ($p \leq 0.07$) between cells adherent on plasma-treated and untreated scaffolds. At 2 hours post-seeding, donor one had little to no cells adhered to the plasma-treated scaffolds and less than 10% of the seeded cells adhered to the untreated scaffolds (Fig. 6). Incubating the cells for longer time periods increased the number of cells that adhered to the PLLA but there was no significant difference between plasma treated and untreated scaffolds. In contrast, plasma treatment significantly increased adhesion by 14.4% ($p = 0.07$) and by 17.6% ($p = 0.03$) at 24 hours post-seeding with cells from donor 2 (Fig. 6). Adhesion of cells from donor 3 was also significantly increased on plasma treated scaffolds by 26.5% at 8 hours ($p = 0.02$). However, the effect of plasma treatment was lost by 12 hours for donor 3 as indicated by the 27.7% increase ($p = 0.07$) in cell adherence on untreated scaffolds (Fig. 6). There was no significant difference between treatments when data for all donors were averaged (Fig. 6). However, two of the three donors did exhibit a greater increase in number of cells when seeded on plasma treated scaffolds, indicating a possibility that plasma treatment of scaffolds may be beneficial.

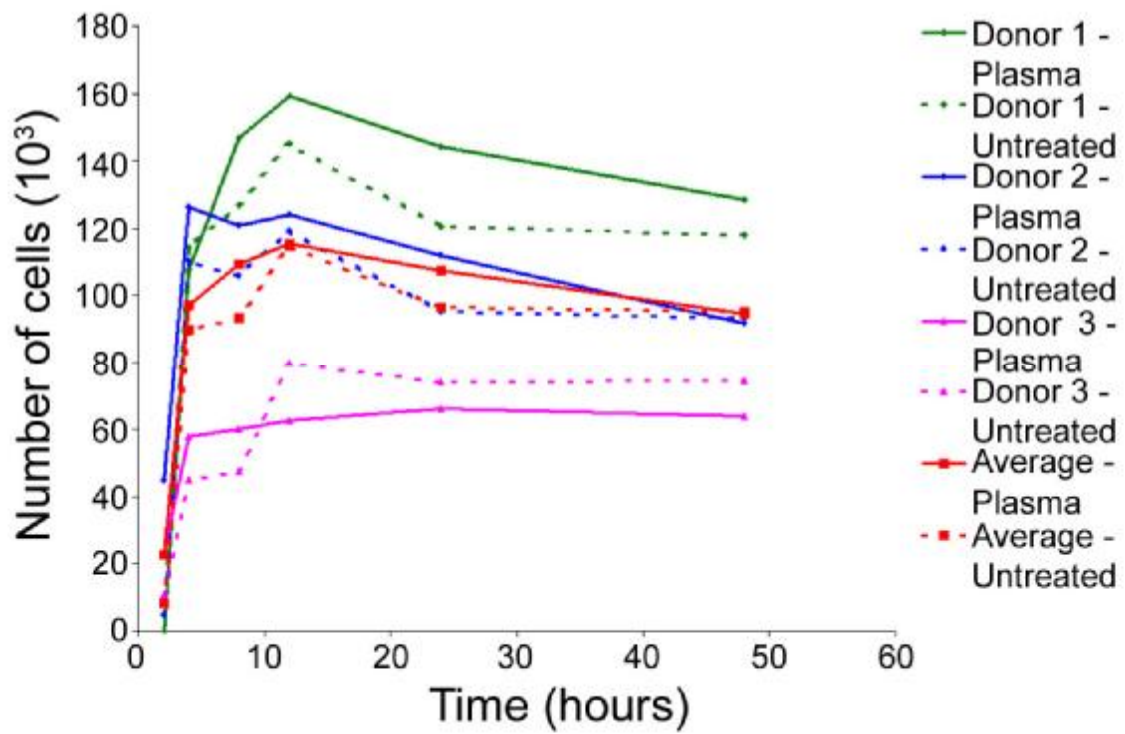


Figure 6. The number of cells that adhered over 48 hours to untreated and oxygen plasma treated PLLA scaffolds based on DNA analysis for all three donors, represented individually and averaged together. Data represent the mean \pm SD.

4. DISCUSSION

Polymers that are typically used in tissue-engineering applications may not be well suited for optimal cellular adhesion and may need to be chemically or physically enhanced. Plasma treatment has been found to improve cellular adhesion by adding functional groups, such as carboxyl or hydroxyl groups, to polymer surfaces. Increased hydrophilicity as a result of adding hydroxyl groups to polyethylene sheets was shown to enhance spreading of Chinese hamster ovary cells [195]. In the present study, oxygen plasma treatment was used to add hydroxyl groups to a PLLA scaffold surface. Plasma treatment resulted in a decreased average contact angle from 75.6° to 58.2° , indicating that the material became more hydrophilic. The contact angle of 58.2° is close to 55° , the angle found to be optimal for cellular adhesion [196]. Lee *et al.* observed that a contact angle of 55° resulted in maximum adhesion and growth of cells, independent of cell type [196]. The present study found that oxygen plasma treatment increased adherence of adipose-derived hMSCs from three donors to melt-blown, non-woven PLLA scaffolds. Furthermore, plasma treatment appeared to enhance cell spreading along PLLA fibers and allowed for a more even distribution of cells through the scaffold at earlier time points when compared to cells in the untreated scaffolds. Taken together, the results of these studies indicate that increasing surface hydrophilicity *via* oxygen plasma treatment can increase the number of adherent hADAS cells to PLLA and can initiate cell spreading at earlier times.

These findings are consistent with those of Nakagawa *et al.* and Yamaguchi *et al.* who found that cell adherence to substrates increased after plasma treatment [184, 185]. Nakagawa *et al.* found that MC3T3-E1 cell activity was greatly enhanced after being seeded on PLLA that had been plasma treated in air or in CO₂ gas [184]. Both cell adhesion and

proliferation were significantly increased when MC3T3-E1 cells were seeded on the plasma-treated surfaces compared to the controls, indicating that the cells preferred the more hydrophilic surface. Yamaguchi *et al.* reported similar findings in a study with Chinese hamster ovary (CHO) cells seeded on oxygen-plasma-treated PLLA films [185]. After 4 hours of incubation, they found an increased number of adherent cells on the plasma-treated films while almost no cells were found on the untreated films. A significant increase in number of cells adherent to plasma-treated PLLA films was observed at 4, 8, 12, and 24 hours.

In addition to the increase in cellular adhesion observed in the present study, plasma treatment of scaffolds prior to cell seeding enhanced distribution of hADAS cells throughout the scaffold and promoted earlier spreading of cells along and across fibers without altering cell viability. The enhanced spreading of cells across the fibers is consistent with findings by Yamaguchi *et al.* who reported that plasma-treated surfaces tended to promote more even cell distribution and initial cell spreading across the scaffold [185]. CHO cells that were seeded and adhered to untreated PLLA films remained separated from one another with a rounded morphology. In comparison, cells seeded on plasma-treated films proliferated closely together to produce a sheet-like structure. In the present study, we also found an early induction of cell spreading and a more uniform distribution of hADAS cells throughout the PLLA scaffold. These effects could have a profound effect in later cell function, specifically for proliferation and differentiation under mechanical stimulation or within *in vivo* environments.

It is known that polymers used for tissue-engineered constructs can modulate hMSC proliferation and differentiation [62]. Recently, it has been shown that scaffold material

composition, as well as pore size, can affect embryonic stem cell hematopoietic differentiation [221]. Additionally, Yang *et al.* found that there was an increase in number of adherent neural stem cells on electrospun, nanofibrous PLLA scaffolds compared to PLLA films [222] indicating that surface architecture can affect cell adhesion. Taken together, these studies emphasize the importance of understanding how substrate surface characteristics (i.e., surface chemistry, composition, and topography) affect not only cell adhesion but also proliferation and differentiation. Understanding how cells act when cultured in a three-dimensional micro- or nanofibrous scaffold will further enable us to engineer more biologically relevant constructs since these scaffolds more closely mimic the natural extracellular matrix [223].

In summary, the present study demonstrated that plasma treatment of non-woven PLLA scaffolds enhanced adhesion, distribution, and spreading of hADAS cells without altering viability. Understanding cellular responses to various treatment conditions, such as oxygen plasma treatment, will aid in determining the optimal conditions necessary for ensuring that hADAS cells remain viable and adherent within tissue-engineered constructs, thus enabling the cells to proliferate and differentiate within the scaffolds and begin to produce their native extracellular matrix.

SUMMARY

Plasma treatment of substrate surfaces can be utilized to improve adhesion of cells to tissue engineered scaffolds. The purpose of this study was to enhance cell adhesion to nonwoven poly (L-lactic acid) (PLLA) scaffolds using oxygen plasma treatment to increase surface hydroxyl groups and thereby enhance substrate hydrophilicity. It was hypothesized that oxygen plasma treatment would increase the number of human adipose-derived adult stem (hADAS) cells that adhered to melt blown, non-woven PLLA scaffolds without affecting cell viability. The number of cells that adhered to the oxygen plasma treated (10 minutes at 100 W) or untreated PLLA scaffolds was assessed at 2, 4, 8, 12, 24, and 48 hours post-seeding via DNA analysis. Cell viability and morphology were also assessed at 2, 4, 8, 12, 24 hours post-seeding via a live/dead assay and hematoxylin staining, respectively. Oxygen plasma treatment decreased the contact angle of water from 75.6° to 58.2° indicating an increase in the surface hydrophilicity of PLLA. The results of the DNA analysis indicated that there was an increased number of hADAS cells on oxygen plasma treated scaffolds for two of the three donors. In addition, oxygen plasma treatment promoted a more even distribution of hADAS cells throughout the scaffold and enhanced cell spreading at earlier time points without altering cell viability. This early induction of cell spreading and the uniform distribution of cells, in turn, may increase future proliferation and differentiation of hADAS cells under conditions that simulate the microenvironment *in vivo*.

CHAPTER 5. CONCLUSIONS

Bone regeneration is a significant area in the field of tissue engineering. The gold standard of treating defective sites is to use autografts or, in the event of limited resources, allografts. Both of these options have limitations and, therefore, tissue engineered bone constructs are being developed that would provide an implant without the disadvantages associated with autografts or allografts. Extensive research has been conducted to produce an optimal bone construct consisting of tissue-specific cells and a biocompatible, mechanically stable scaffold. While there are commercially available products that provide some of these components, an optimal combination has yet to be developed. In order to successfully produce a bone construct that can repair or regenerate lost or defective tissue, a better understanding of cell differentiation and cell-scaffold interactions are needed.

The first study presented in this thesis investigated the response of hADAS cells from donors of varying osteogenic differentiation capabilities to mechanical loading, both continuous and rest inserted, as compared to unstrained controls. Human ADAS cells from both donors, one high calcium producer and another low calcium producer, increased their calcium deposition in response to mechanical loading compared to unstrained controls. This suggests that mechanical stimulation can be used to enhance the osteogenic differentiation of hADAS cells from a poor producing calcium donor, regardless of its original capability. However, hADAS cells from a donor who innately produces calcium well responded more positively to mechanical stimulation than the donor cells that deposited low quantities of calcium. It is apparent from these results that mechanical stimulation is a key component to the osteogenic differentiation of hADAS cells, similar to reports done with bone marrow-derived mesenchymal stem cells.

Cell-scaffold interactions are another important component to the success of tissue engineered bone constructs. Cell adhesion to the scaffold is necessary for cells' future proliferation, differentiation, and subsequent tissue development. The second study presented in Chapter 4 of this thesis investigated the use of oxygen plasma to enhance the adhesion efficiency, and early cell morphology and distribution. The hydroxyl groups added to the surface of the non-woven PLLA scaffold significantly increased the number of cells which adhered to the scaffolds for 2 of the 3 donors, signifying the positive cell response to increased hydrophilicity of a material. In addition, cells seeded on plasma treated scaffolds had increased early cell spreading and distribution compared to cells seeded on untreated scaffolds. The enhanced early cell spreading and distribution due to oxygen plasma treatment of synthetic PLLA scaffolds suggest that this methodology can be used to produce a more optimal procedure of creating tissue engineered bone grafts.

Future Directions

From studies investigating the differentiation potential of bone marrow-derived stem cells compared to adipose-derived stem cells, it is obvious that mesenchymal stem cells from different sources do not respond identically to the same stimuli. Results from the first study reported in this thesis (Chapter 2) show that the response of hADAS cells to rest inserted loading compared to continuous loading did not correspond to those documented by other investigators using other cell lines; this suggests that the mechanisms involved in the differentiation of hADAS cells might be different than mesenchymal stem cells from other sources, bone progenitor cells and osteoblasts. Therefore, results found from studies evaluating rest insertion loading using cells from other sources may not be fully applicable to

ADAS cells. Consequently, further investigation is needed to investigate the mechanisms associated with the differentiation of ADAS cells, specifically those that are dampened during continuous loading and become desensitized.

While tensile strain has shown to be a successful method for inducing osteogenic differentiation of MSCs, there is also evidence that fluid shear stress may be a more effective and appropriate method for osteogenesis. Recent published studies that have compared the responsiveness of bone cells to tensile strain and fluid shear stress have found that different intracellular mechanisms are triggered depending on the type of mechanical loading. More importantly, higher protein expression and Ca^{2+} signaling are reported when bone cells experience fluid shear stress as opposed to mechanical strain. It is this reason why studies involving the using of fluid shear stress to induce osteogenesis of MSCs have become ever increasingly popular.

This shift from using tensile strain as the optimal method to mechanically induce osteogenesis towards using fluid shear stress has created the need to develop fluid shear bioreactors. Fluid shear bioreactors rely on well seeded, porous, three-dimensional scaffolds in order to induce differentiation of cells via fluid shear stress as well as provide nutrient delivery and waste removal. The results presented in the study investigating the cellular adhesion response to oxygen plasma treated PLLA scaffolds (Chapter 4) have important implications for optimizing the development of a bone graft. By achieving early cell spreading within and throughout a scaffold, this may allow for stronger adhesion to scaffold fibers. In turn, this may allow for cells to be subjected to higher shear stresses and thus, enhanced differentiation. Additionally, early cell spreading allows for more of the cell

membrane to be exposed to the fluid shear stress and therefore more mechanically sensitive channels can be activated via fluid flow.

Although there is a move towards using fluid shear stress for osteogenesis as opposed to tensile strain, the information gathered from studies utilizing tensile strain is still applicable for future studies using fluid shear stress. The desensitization of bone cells and osteoblasts from continual mechanical loading is a phenomenon that will still occur under fluid shear stress. Thus, future research into osteogenesis of hADAS cells in macro and microfluidic bioreactors should still apply the same principles when applying mechanical loading regimens.

LITERATURE CITED

1. Currey, J.D., *Bones*. 2002, Princeton: Princeton University Press.
2. Marks, S., Hermey, DC, *The Structure and Development of Bone*, in *Principles of Bone Biology*, J. Bilezikian, Raisz, LG, Rodan, GA, Editor. 1996, Academic Press: San Diego. p. 3-14.
3. Guilak, F., DL Butler, SA Goldstein, DJ Mooney, ed. *Functional tissue engineering*. 2003, Springer-Verlag: New York.
4. Sikavitsas, V.I., J.S. Temenoff, and A.G. Mikos, *Biomaterials and bone mechanotransduction*. *Biomaterials*, 2001. **22**(19): p. 2581-93.
5. Buckwalter, J.A., et al., *Bone biology. I: Structure, blood supply, cells, matrix, and mineralization*. *Instr Course Lect*, 1996. **45**: p. 371-86.
6. Nijweide, P., Burger, EH, Nulend, JK, Van der Plas, A., *The Osteocyte*, in *Principles of Bone Biology*, J. Bilezikian, Raisz, LG, Rodan, GA, Editor. 1996, Academic Press, Inc: San Diego. p. 115-126.
7. Cowin, S.C., L. Moss-Salentijn, and M.L. Moss, *Candidates for the mechanosensory system in bone*. *J Biomech Eng*, 1991. **113**(2): p. 191-7.
8. Vaananen, K., *Osteoclast Function: Biology and Mechanisms*, in *Principles of Bone Biology*, J. Bilezikian, Raisz, LG, Rodan, GA, Editor. 1996, Academic Press, Inc.: San Diego. p. 103-113.
9. Klein-Nulend, J., CM Semeins, EH Burger, A Van der Plas, NE Ajubi, PJ Nijweide., *Response of isolated osteocytes to mechanical loading in vitro*, in *Bone Structure and Remodeling*, A. Odgaard, Weinans, H, Editor. 1994, World Scientific Publishing Co. Pte. Ltd. p. 37-49.
10. Duncan, R.L. and C.H. Turner, *Mechanotransduction and the functional response of bone to mechanical strain*. *Calcif Tissue Int*, 1995. **57**(5): p. 344-58.
11. Carter, D.R., et al., *Mechanobiology of skeletal regeneration*. *Clin Orthop Relat Res*, 1998(355 Suppl): p. S41-55.
12. Rubin, J., C. Rubin, and C.R. Jacobs, *Molecular pathways mediating mechanical signaling in bone*. *Gene*, 2006. **367**: p. 1-16.
13. Knothe Tate, M.L., *"Whither flows the fluid in bone?" An osteocyte's perspective*. *J Biomech*, 2003. **36**(10): p. 1409-24.

14. Burger, E.H. and J. Klein-Nulend, *Mechanotransduction in bone--role of the lacuno-canalicular network*. *Faseb J*, 1999. **13 Suppl**: p. S101-12.
15. Rubin, C.T. and L.E. Lanyon, *Regulation of bone formation by applied dynamic loads*. *J Bone Joint Surg Am*, 1984. **66**(3): p. 397-402.
16. Weinbaum, S., S.C. Cowin, and Y. Zeng, *A model for the excitation of osteocytes by mechanical loading-induced bone fluid shear stresses*. *J Biomech*, 1994. **27**(3): p. 339-60.
17. Burger, E.H. and J. Klein-Nulend, *Responses of bone cells to biomechanical forces in vitro*. *Adv Dent Res*, 1999. **13**: p. 93-8.
18. Mullender, M., et al., *Mechanotransduction of bone cells in vitro: mechanobiology of bone tissue*. *Med Biol Eng Comput*, 2004. **42**(1): p. 14-21.
19. Ajubi, N.E., et al., *Pulsating fluid flow increases prostaglandin production by cultured chicken osteocytes--a cytoskeleton-dependent process*. *Biochem Biophys Res Commun*, 1996. **225**(1): p. 62-8.
20. Klein-Nulend, J., et al., *Sensitivity of osteocytes to biomechanical stress in vitro*. *Faseb J*, 1995. **9**(5): p. 441-5.
21. Klein-Nulend, J., et al., *Pulsating fluid flow increases nitric oxide (NO) synthesis by osteocytes but not periosteal fibroblasts--correlation with prostaglandin upregulation*. *Biochem Biophys Res Commun*, 1995. **217**(2): p. 640-8.
22. Banes, A.J., et al., *Mechanical forces and signaling in connective tissue cells: cellular mechanisms of detection, transduction, and responses to mechanical deformation*. *Current Opinion in Orthopaedics*, 2001. **12**: p. 389-396.
23. Ingber, D.E., *Tensegrity: the architectural basis of cellular mechanotransduction*. *Annu Rev Physiol*, 1997. **59**: p. 575-99.
24. Ingber, D.E. and J. Folkman, *Mechanochemical switching between growth and differentiation during fibroblast growth factor-stimulated angiogenesis in vitro: role of extracellular matrix*. *J Cell Biol*, 1989. **109**(1): p. 317-30.
25. Rana, B., et al., *Cell-extracellular matrix interactions can regulate the switch between growth and differentiation in rat hepatocytes: reciprocal expression of C/EBP alpha and immediate-early growth response transcription factors*. *Mol Cell Biol*, 1994. **14**(9): p. 5858-69.
26. Mooney, D., et al., *Switching from differentiation to growth in hepatocytes: control by extracellular matrix*. *J Cell Physiol*, 1992. **151**(3): p. 497-505.

27. Hansen, L.K., et al., *Integrin binding and cell spreading on extracellular matrix act at different points in the cell cycle to promote hepatocyte growth*. Mol Biol Cell, 1994. **5**(9): p. 967-75.
28. McGarry, J.G., J. Klein-Nulend, and P.J. Prendergast, *The effect of cytoskeletal disruption on pulsatile fluid flow-induced nitric oxide and prostaglandin E2 release in osteocytes and osteoblasts*. Biochem Biophys Res Commun, 2005. **330**(1): p. 341-8.
29. Pavalko, F.M., et al., *Fluid shear-induced mechanical signaling in MC3T3-E1 osteoblasts requires cytoskeleton-integrin interactions*. Am J Physiol, 1998. **275**(6 Pt 1): p. C1591-601.
30. Rawlinson, S.C., A.A. Pitsillides, and L.E. Lanyon, *Involvement of different ion channels in osteoblasts' and osteocytes' early responses to mechanical strain*. Bone, 1996. **19**(6): p. 609-14.
31. Charras, G.T., et al., *Estimating the sensitivity of mechanosensitive ion channels to membrane strain and tension*. Biophys J, 2004. **87**(4): p. 2870-84.
32. Davidson, R.M., *Membrane stretch activates a high-conductance K⁺ channel in G292 osteoblastic-like cells*. J Membr Biol, 1993. **131**(1): p. 81-92.
33. Davidson, R.M., D.W. Tatakis, and A.L. Auerbach, *Multiple forms of mechanosensitive ion channels in osteoblast-like cells*. Pflugers Arch, 1990. **416**(6): p. 646-51.
34. Li, J., et al., *L-type calcium channels mediate mechanically induced bone formation in vivo*. J Bone Miner Res, 2002. **17**(10): p. 1795-800.
35. Jiang, J.X., A.J. Siller-Jackson, and S. Burra, *Roles of gap junctions and hemichannels in bone cell functions and in signal transmission of mechanical stress*. Front Biosci, 2007. **12**: p. 1450-62.
36. Taylor, A.F., et al., *Mechanically stimulated osteocytes regulate osteoblastic activity via gap junctions*. Am J Physiol Cell Physiol, 2007. **292**(1): p. C545-52.
37. Gilbert, S.F., *Developmental Biology*. Fourth ed. 1994, Sunderland: Sinauer Associates, Inc.
38. Alberts, B., Johnson, A, Lewis, J, Raff, M, Roberts, K, Walter, P, ed. *Molecular biology of the cell*. Fourth Edition ed. 2002, Garland Science: New York.
39. Brehm, M., T. Zeus, and B.E. Strauer, *Stem cells--clinical application and perspectives*. Herz, 2002. **27**(7): p. 611-20.
40. Pittenger, M.F., et al., *Multilineage potential of adult human mesenchymal stem cells*. Science, 1999. **284**(5411): p. 143-7.

41. De Ugarte, D.A., et al., *Comparison of multi-lineage cells from human adipose tissue and bone marrow*. Cells Tissues Organs, 2003. **174**(3): p. 101-9.
42. Huang, G.P., et al., *Ex vivo expansion and transplantation of hematopoietic stem/progenitor cells supported by mesenchymal stem cells from human umbilical cord blood*. Cell Transplant, 2007. **16**(6): p. 579-85.
43. Zvaifler, N.J., et al., *Mesenchymal precursor cells in the blood of normal individuals*. Arthritis Res, 2000. **2**(6): p. 477-88.
44. De Coppi, P., et al., *Isolation of amniotic stem cell lines with potential for therapy*. Nat Biotechnol, 2007. **25**(1): p. 100-6.
45. Kim, J., et al., *Human amniotic fluid-derived stem cells have characteristics of multipotent stem cells*. Cell Prolif, 2007. **40**(1): p. 75-90.
46. Guilak, F., et al., *Clonal analysis of the differentiation potential of human adipose-derived adult stem cells*. J Cell Physiol, 2006. **206**(1): p. 229-37.
47. Zuk, P.A., et al., *Human adipose tissue is a source of multipotent stem cells*. Mol Biol Cell, 2002. **13**(12): p. 4279-95.
48. Zuk, P.A., et al., *Multilineage cells from human adipose tissue: implications for cell-based therapies*. Tissue Eng, 2001. **7**(2): p. 211-28.
49. Strem, B.M., et al., *Multipotential differentiation of adipose tissue-derived stem cells*. Keio J Med, 2005. **54**(3): p. 132-41.
50. De Ugarte, D.A., et al., *Differential expression of stem cell mobilization-associated molecules on multi-lineage cells from adipose tissue and bone marrow*. Immunol Lett, 2003. **89**(2-3): p. 267-70.
51. Wall, M.E., S.H. Bernacki, and E.G. Lobo, *Effects of serial passaging on the adipogenic and osteogenic differentiation potential of adipose-derived human mesenchymal stem cells*. Tissue Eng, 2007. **13**(6): p. 1291-8.
52. Sumanasinghe, R.D., S.H. Bernacki, and E.G. Lobo, *Osteogenic differentiation of human mesenchymal stem cells in collagen matrices: effect of uniaxial cyclic tensile strain on bone morphogenetic protein (BMP-2) mRNA expression*. Tissue Eng, 2006. **12**(12): p. 3459-65.
53. Endres, M., et al., *Osteogenic induction of human bone marrow-derived mesenchymal progenitor cells in novel synthetic polymer-hydrogel matrices*. Tissue Eng, 2003. **9**(4): p. 689-702.

54. Im, G.I., Y.W. Shin, and K.B. Lee, *Do adipose tissue-derived mesenchymal stem cells have the same osteogenic and chondrogenic potential as bone marrow-derived cells?* Osteoarthritis Cartilage, 2005. **13**(10): p. 845-53.
55. Weinzierl, K., A. Hemprich, and B. Frerich, *Bone engineering with adipose tissue derived stromal cells.* J Craniomaxillofac Surg, 2006. **34**(8): p. 466-71.
56. Engler, A.J., et al., *Matrix elasticity directs stem cell lineage specification.* Cell, 2006. **126**(4): p. 677-89.
57. Mauney, J.R., et al., *Mechanical stimulation promotes osteogenic differentiation of human bone marrow stromal cells on 3-D partially demineralized bone scaffolds in vitro.* Calcif Tissue Int, 2004. **74**(5): p. 458-68.
58. Ward, D.F., Jr., et al., *Mechanical strain enhances extracellular matrix-induced gene focusing and promotes osteogenic differentiation of human mesenchymal stem cells through an extracellular-related kinase-dependent pathway.* Stem Cells Dev, 2007. **16**(3): p. 467-80.
59. Li, Y.J., et al., *Oscillatory fluid flow affects human marrow stromal cell proliferation and differentiation.* J Orthop Res, 2004. **22**(6): p. 1283-9.
60. Halvorsen, Y.D., et al., *Extracellular matrix mineralization and osteoblast gene expression by human adipose tissue-derived stromal cells.* Tissue Eng, 2001. **7**(6): p. 729-41.
61. Bancroft, G.N., et al., *Fluid flow increases mineralized matrix deposition in 3D perfusion culture of marrow stromal osteoblasts in a dose-dependent manner.* Proc Natl Acad Sci U S A, 2002. **99**(20): p. 12600-5.
62. Jager, M., et al., *Proliferation and osteogenic differentiation of mesenchymal stem cells cultured onto three different polymers in vitro.* Ann Biomed Eng, 2005. **33**(10): p. 1319-32.
63. Mauney, J.R., et al., *Engineering adipose-like tissue in vitro and in vivo utilizing human bone marrow and adipose-derived mesenchymal stem cells with silk fibroin 3D scaffolds.* Biomaterials, 2007.
64. Sen, A., et al., *Adipogenic potential of human adipose derived stromal cells from multiple donors is heterogeneous.* J Cell Biochem, 2001. **81**(2): p. 312-9.
65. Wakitani, S., et al., *Mesenchymal cell-based repair of large, full-thickness defects of articular cartilage.* J Bone Joint Surg Am, 1994. **76**(4): p. 579-92.
66. Saitoh, S., et al., *Compressive force promotes chondrogenic differentiation and hypertrophy in midpalatal suture cartilage in growing rats.* Anat Rec, 2000. **260**(4): p. 392-401.

67. Mehlhorn, A.T., et al., *Differential expression pattern of extracellular matrix molecules during chondrogenesis of mesenchymal stem cells from bone marrow and adipose tissue*. Tissue Eng, 2006. **12**(10): p. 2853-62.
68. Afizah, H., et al., *A comparison between the chondrogenic potential of human bone marrow stem cells (BMSCs) and adipose-derived stem cells (ADSCs) taken from the same donors*. Tissue Eng, 2007. **13**(4): p. 659-66.
69. Yang, G., R.C. Crawford, and J.H. Wang, *Proliferation and collagen production of human patellar tendon fibroblasts in response to cyclic uniaxial stretching in serum-free conditions*. J Biomech, 2004. **37**(10): p. 1543-50.
70. Young, R.G., et al., *Use of mesenchymal stem cells in a collagen matrix for Achilles tendon repair*. J Orthop Res, 1998. **16**(4): p. 406-13.
71. Lee, I.C., et al., *The differentiation of mesenchymal stem cells by mechanical stress or/and co-culture system*. Biochem Biophys Res Commun, 2007. **352**(1): p. 147-52.
72. Park, J.S., et al., *Differential effects of equiaxial and uniaxial strain on mesenchymal stem cells*. Biotechnol Bioeng, 2004. **88**(3): p. 359-68.
73. Sanchez-Ramos, J., et al., *Adult bone marrow stromal cells differentiate into neural cells in vitro*. Exp Neurol, 2000. **164**(2): p. 247-56.
74. Arinzeh, T.L., et al., *Allogeneic mesenchymal stem cells regenerate bone in a critical-sized canine segmental defect*. J Bone Joint Surg Am, 2003. **85-A**(10): p. 1927-35.
75. Schantz, J.T., et al., *Repair of calvarial defects with customised tissue-engineered bone grafts II. Evaluation of cellular efficiency and efficacy in vivo*. Tissue Eng, 2003. **9 Suppl 1**: p. S127-39.
76. Bruder, S.P., et al., *The effect of implants loaded with autologous mesenchymal stem cells on the healing of canine segmental bone defects*. J Bone Joint Surg Am, 1998. **80**(7): p. 985-96.
77. Aust, L., et al., *Yield of human adipose-derived adult stem cells from liposuction aspirates*. Cytotherapy, 2004. **6**(1): p. 7-14.
78. Hattori, H., et al., *Osteogenic potential of human adipose tissue-derived stromal cells as an alternative stem cell source*. Cells Tissues Organs, 2004. **178**(1): p. 2-12.
79. Vidal, M.A., et al., *Characterization of equine adipose tissue-derived stromal cells: adipogenic and osteogenic capacity and comparison with bone marrow-derived mesenchymal stromal cells*. Vet Surg, 2007. **36**(7): p. 613-22.

80. Liu, T.M., et al., *Identification of common pathways mediating differentiation of bone marrow- and adipose tissue-derived human mesenchymal stem cells into three mesenchymal lineages*. *Stem Cells*, 2007. **25**(3): p. 750-60.
81. Estes, B.T., A.W. Wu, and F. Guilak, *Potent induction of chondrocytic differentiation of human adipose-derived adult stem cells by bone morphogenetic protein 6*. *Arthritis Rheum*, 2006. **54**(4): p. 1222-32.
82. Estes, B.T., et al., *Extended passaging, but not aldehyde dehydrogenase activity, increases the chondrogenic potential of human adipose-derived adult stem cells*. *J Cell Physiol*, 2006. **209**(3): p. 987-95.
83. Younger, E.M. and M.W. Chapman, *Morbidity at bone graft donor sites*. *J Orthop Trauma*, 1989. **3**(3): p. 192-5.
84. Ringe, J., et al., *Stem cells for regenerative medicine: advances in the engineering of tissues and organs*. *Naturwissenschaften*, 2002. **89**(8): p. 338-51.
85. Moore, W.R., S.E. Graves, and G.I. Bain, *Synthetic bone graft substitutes*. *ANZ J Surg*, 2001. **71**(6): p. 354-61.
86. Hui, J.H., et al., *Mesenchymal stem cells in musculoskeletal tissue engineering: a review of recent advances in National University of Singapore*. *Ann Acad Med Singapore*, 2005. **34**(2): p. 206-12.
87. Bonassar, L.J. and C.A. Vacanti, *Tissue engineering: the first decade and beyond*. *J Cell Biochem Suppl*, 1998. **30-31**: p. 297-303.
88. Vacanti, C.A. and J.P. Vacanti, *The science of tissue engineering*. *Orthop Clin North Am*, 2000. **31**(3): p. 351-6.
89. Quarto, R., et al., *Repair of large bone defects with the use of autologous bone marrow stromal cells*. *N Engl J Med*, 2001. **344**(5): p. 385-6.
90. Kon, E., et al., *Autologous bone marrow stromal cells loaded onto porous hydroxyapatite ceramic accelerate bone repair in critical-size defects of sheep long bones*. *J Biomed Mater Res*, 2000. **49**(3): p. 328-37.
91. Liu, Y., X.Z. Shu, and G.D. Prestwich, *Osteochondral defect repair with autologous bone marrow-derived mesenchymal stem cells in an injectable, in situ, cross-linked synthetic extracellular matrix*. *Tissue Eng*, 2006. **12**(12): p. 3405-16.
92. Yan, H. and C. Yu, *Repair of full-thickness cartilage defects with cells of different origin in a rabbit model*. *Arthroscopy*, 2007. **23**(2): p. 178-87.

93. Kuroda, R., et al., *Treatment of a full-thickness articular cartilage defect in the femoral condyle of an athlete with autologous bone-marrow stromal cells*. Osteoarthritis Cartilage, 2007. **15**(2): p. 226-31.
94. Wakitani, S., et al., *Human autologous culture expanded bone marrow mesenchymal cell transplantation for repair of cartilage defects in osteoarthritic knees*. Osteoarthritis Cartilage, 2002. **10**(3): p. 199-206.
95. Juncosa-Melvin, N., et al., *Effects of mechanical stimulation on the biomechanics and histology of stem cell-collagen sponge constructs for rabbit patellar tendon repair*. Tissue Eng, 2006. **12**(8): p. 2291-300.
96. Awad, H.A., et al., *Repair of patellar tendon injuries using a cell-collagen composite*. J Orthop Res, 2003. **21**(3): p. 420-31.
97. Cheng, S.L., et al., *Differentiation of human bone marrow osteogenic stromal cells in vitro: induction of the osteoblast phenotype by dexamethasone*. Endocrinology, 1994. **134**(1): p. 277-86.
98. Ringe, J., et al., *Porcine mesenchymal stem cells. Induction of distinct mesenchymal cell lineages*. Cell Tissue Res, 2002. **307**(3): p. 321-7.
99. Jorgensen, N.R., et al., *Dexamethasone, BMP-2, and 1,25-dihydroxyvitamin D enhance a more differentiated osteoblast phenotype: validation of an in vitro model for human bone marrow-derived primary osteoblasts*. Steroids, 2004. **69**(4): p. 219-26.
100. Nuttelman, C.R., M.C. Tripodi, and K.S. Anseth, *Dexamethasone-functionalized gels induce osteogenic differentiation of encapsulated hMSCs*. J Biomed Mater Res A, 2006. **76**(1): p. 183-95.
101. Karageorgiou, V., et al., *Bone morphogenetic protein-2 decorated silk fibroin films induce osteogenic differentiation of human bone marrow stromal cells*. J Biomed Mater Res A, 2004. **71**(3): p. 528-37.
102. Jaiswal, N., et al., *Osteogenic differentiation of purified, culture-expanded human mesenchymal stem cells in vitro*. J Cell Biochem, 1997. **64**(2): p. 295-312.
103. Raab-Cullen, D.M., et al., *Bone response to alternate-day mechanical loading of the rat tibia*. J Bone Miner Res, 1994. **9**(2): p. 203-11.
104. Zhao, F., R. Chella, and T. Ma, *Effects of shear stress on 3-D human mesenchymal stem cell construct development in a perfusion bioreactor system: Experiments and hydrodynamic modeling*. Biotechnol Bioeng, 2007. **96**(3): p. 584-95.
105. Cartmell, S.H., et al., *Effects of medium perfusion rate on cell-seeded three-dimensional bone constructs in vitro*. Tissue Eng, 2003. **9**(6): p. 1197-203.

106. Goldstein, A.S., et al., *Effect of convection on osteoblastic cell growth and function in biodegradable polymer foam scaffolds*. *Biomaterials*, 2001. **22**(11): p. 1279-88.
107. Kim, S.G., et al., *Gene expression of type I and type III collagen by mechanical stretch in anterior cruciate ligament cells*. *Cell Struct Funct*, 2002. **27**(3): p. 139-44.
108. Meyer, U., et al., *Strain-related bone remodeling in distraction osteogenesis of the mandible*. *Plast Reconstr Surg*, 1999. **103**(3): p. 800-7.
109. Frost, H.M., *Skeletal structural adaptations to mechanical usage (SATMU): 1. Redefining Wolff's law: the bone modeling problem*. *Anat Rec*, 1990. **226**(4): p. 403-13.
110. Frost, H.M., *Bone "mass" and the "mechanostat": a proposal*. *Anat Rec*, 1987. **219**(1): p. 1-9.
111. Loba, E.G., et al., *Mechanobiology of mandibular distraction osteogenesis: experimental analyses with a rat model*. *Bone*, 2004. **34**(2): p. 336-43.
112. Richards, M., et al., *Bone regeneration and fracture healing. Experience with distraction osteogenesis model*. *Clin Orthop Relat Res*, 1998(355 Suppl): p. S191-204.
113. Waanders, N.A., et al., *Evaluation of the mechanical environment during distraction osteogenesis*. *Clin Orthop Relat Res*, 1998(349): p. 225-34.
114. Smith-Adaline, E.A., et al., *Mechanical environment alters tissue formation patterns during fracture repair*. *J Orthop Res*, 2004. **22**(5): p. 1079-85.
115. Simmons, C.A., et al., *Cyclic strain enhances matrix mineralization by adult human mesenchymal stem cells via the extracellular signal-regulated kinase (ERK1/2) signaling pathway*. *J Biomech*, 2003. **36**(8): p. 1087-96.
116. Ignatius, A., et al., *Tissue engineering of bone: effects of mechanical strain on osteoblastic cells in type I collagen matrices*. *Biomaterials*, 2005. **26**(3): p. 311-8.
117. Kaspar, D., et al., *Proliferation of human-derived osteoblast-like cells depends on the cycle number and frequency of uniaxial strain*. *J Biomech*, 2002. **35**(7): p. 873-80.
118. Qin, Y.X., C.T. Rubin, and K.J. McLeod, *Nonlinear dependence of loading intensity and cycle number in the maintenance of bone mass and morphology*. *J Orthop Res*, 1998. **16**(4): p. 482-9.
119. Turner, C.H., *Three rules for bone adaptation to mechanical stimuli*. *Bone*, 1998. **23**(5): p. 399-407.
120. Umemura, Y., et al., *Five jumps per day increase bone mass and breaking force in rats*. *J Bone Miner Res*, 1997. **12**(9): p. 1480-5.

121. Robling, A.G., D.B. Burr, and C.H. Turner, *Recovery periods restore mechanosensitivity to dynamically loaded bone*. J Exp Biol, 2001. **204**(Pt 19): p. 3389-99.
122. Srinivasan, S., et al., *Rest-inserted loading rapidly amplifies the response of bone to small increases in strain and load cycles*. J Appl Physiol, 2007. **102**(5): p. 1945-52.
123. Srinivasan, S., et al., *Enabling bone formation in the aged skeleton via rest-inserted mechanical loading*. Bone, 2003. **33**(6): p. 946-55.
124. LaMothe, J.M. and R.F. Zernicke, *Rest insertion combined with high-frequency loading enhances osteogenesis*. J Appl Physiol, 2004. **96**(5): p. 1788-93.
125. Robling, A.G., D.B. Burr, and C.H. Turner, *Partitioning a daily mechanical stimulus into discrete loading bouts improves the osteogenic response to loading*. J Bone Miner Res, 2000. **15**(8): p. 1596-602.
126. Srinivasan, S., et al., *Low-magnitude mechanical loading becomes osteogenic when rest is inserted between each load cycle*. J Bone Miner Res, 2002. **17**(9): p. 1613-20.
127. Batra, N.N., et al., *Effects of short-term recovery periods on fluid-induced signaling in osteoblastic cells*. J Biomech, 2005. **38**(9): p. 1909-17.
128. Donahue, S.W., H.J. Donahue, and C.R. Jacobs, *Osteoblastic cells have refractory periods for fluid-flow-induced intracellular calcium oscillations for short bouts of flow and display multiple low-magnitude oscillations during long-term flow*. J Biomech, 2003. **36**(1): p. 35-43.
129. Paccione, M.F., et al., *Rat mandibular distraction osteogenesis: latency, rate, and rhythm determine the adaptive response*. J Craniofac Surg, 2001. **12**(2): p. 175-82.
130. Siddappa, R., et al., *Donor variation and loss of multipotency during in vitro expansion of human mesenchymal stem cells for bone tissue engineering*. J Orthop Res, 2007. **25**(8): p. 1029-41.
131. Phinney, D.G., et al., *Donor variation in the growth properties and osteogenic potential of human marrow stromal cells*. J Cell Biochem, 1999. **75**(3): p. 424-36.
132. Hanson, A., ME Wall, B Pourdeyhimi, EG Lobo, *Effects of oxygen plasma treatment on adipose-derived human mesenchymal stem cell adherence to poly(L-lactic acid) scaffolds*. Journal of Biomaterial Science. Polymer Edition., 2007. **18**(11): p. 1387-1400.
133. Awad, H.A., et al., *Effects of transforming growth factor beta1 and dexamethasone on the growth and chondrogenic differentiation of adipose-derived stromal cells*. Tissue Eng, 2003. **9**(6): p. 1301-12.
134. *AlamarBlue*, T. Datasheet, Editor. 2002, AbD Serotec Ltd.: Kidlington.

135. Klein, B.Y., I. Gal, and D. Segal, *Marrow stromal cell commitment to mineralization under the effect of a prolyl hydroxylase inhibitor*. J Cell Biochem, 1994. **54**(3): p. 354-64.
136. Cypher, T.J. and J.P. Grossman, *Biological principles of bone graft healing*. J Foot Ankle Surg, 1996. **35**(5): p. 413-7.
137. Ahlmann, E., et al., *Comparison of anterior and posterior iliac crest bone grafts in terms of harvest-site morbidity and functional outcomes*. J Bone Joint Surg Am, 2002. **84-A**(5): p. 716-20.
138. Sasso, R.C., J.C. LeHuec, and C. Shaffrey, *Iliac crest bone graft donor site pain after anterior lumbar interbody fusion: a prospective patient satisfaction outcome assessment*. J Spinal Disord Tech, 2005. **18 Suppl**: p. S77-81.
139. Seiler, J.G., 3rd and J. Johnson, *Iliac crest autogenous bone grafting: donor site complications*. J South Orthop Assoc, 2000. **9**(2): p. 91-7.
140. Friedlaender, G.E., et al., *Long-term follow-up of patients with osteochondral allografts. A correlation between immunologic responses and clinical outcome*. Orthop Clin North Am, 1999. **30**(4): p. 583-8.
141. Pelker, R.R. and G.E. Friedlaender, *Biomechanical aspects of bone autografts and allografts*. Orthop Clin North Am, 1987. **18**(2): p. 235-9.
142. Hutmacher, D.W., *Scaffolds in tissue engineering bone and cartilage*. Biomaterials, 2000. **21**(24): p. 2529-43.
143. Karageorgiou, V. and D. Kaplan, *Porosity of 3D biomaterial scaffolds and osteogenesis*. Biomaterials, 2005. **26**(27): p. 5474-91.
144. Robinson, B.P., et al., *Calvarial bone repair with porous D,L-poly lactide*. Otolaryngol Head Neck Surg, 1995. **112**(6): p. 707-13.
145. Athanasiou, K.A., et al., *Fundamentals of biomechanics in tissue engineering of bone*. Tissue Eng, 2000. **6**(4): p. 361-81.
146. Keaveny, T.M., et al., *Biomechanics of trabecular bone*. Annu Rev Biomed Eng, 2001. **3**: p. 307-33.
147. Colton, C.K., *Implantable biohybrid artificial organs*. Cell Transplant, 1995. **4**(4): p. 415-36.
148. Klenke, F.M., et al., *Impact of pore size on the vascularization and osseointegration of ceramic bone substitutes in vivo*. J Biomed Mater Res A, 2007.
149. Takahashi, Y. and Y. Tabata, *Effect of the fiber diameter and porosity of non-woven PET fabrics on the osteogenic differentiation of mesenchymal stem cells*. J Biomater Sci Polym Ed, 2004. **15**(1): p. 41-57.

150. Bignon, A., et al., *Effect of micro- and macroporosity of bone substitutes on their mechanical properties and cellular response*. J Mater Sci Mater Med, 2003. **14**(12): p. 1089-97.
151. Borden, M., et al., *Structural and human cellular assessment of a novel microsphere-based tissue engineered scaffold for bone repair*. Biomaterials, 2003. **24**(4): p. 597-609.
152. Yang, S., et al., *The design of scaffolds for use in tissue engineering. Part I. Traditional factors*. Tissue Eng, 2001. **7**(6): p. 679-89.
153. Shalaby, S., *Fabrics*, in *Biomaterials Science: An introduction to materials in medicine*, B. Ratner, Hoffman, AS, Schoen, FJ, Lemons, JE, Editor. 1996, Academic Press: San Diego. p. 118-124.
154. Mano, J.F., et al., *Natural origin biodegradable systems in tissue engineering and regenerative medicine: present status and some moving trends*. J R Soc Interface, 2007.
155. Kakudo, N., et al., *Bone tissue engineering using human adipose-derived stem cells and honeycomb collagen scaffold*. J Biomed Mater Res A, 2007.
156. Shih, Y.R., et al., *Growth of mesenchymal stem cells on electrospun type I collagen nanofibers*. Stem Cells, 2006. **24**(11): p. 2391-7.
157. Jiang, T., W.I. Abdel-Fattah, and C.T. Laurencin, *In vitro evaluation of chitosan/poly(lactic acid-glycolic acid) sintered microsphere scaffolds for bone tissue engineering*. Biomaterials, 2006. **27**(28): p. 4894-903.
158. Di Martino, A., M. Sittinger, and M.V. Risbud, *Chitosan: a versatile biopolymer for orthopaedic tissue-engineering*. Biomaterials, 2005. **26**(30): p. 5983-90.
159. Kim, I.Y., et al., *Chitosan and its derivatives for tissue engineering applications*. Biotechnol Adv, 2007.
160. Hasegawa, S., et al., *In vivo evaluation of a porous hydroxyapatite/poly-DL-lactide composite for bone tissue engineering*. J Biomed Mater Res A, 2007. **81**(4): p. 930-8.
161. Shor, L., et al., *Fabrication of three-dimensional polycaprolactone/hydroxyapatite tissue scaffolds and osteoblast-scaffold interactions in vitro*. Biomaterials, 2007. **28**(35): p. 5291-7.
162. Acarturk, T.O. and J.O. Hollinger, *Commercially available demineralized bone matrix compositions to regenerate calvarial critical-sized bone defects*. Plast Reconstr Surg, 2006. **118**(4): p. 862-73.
163. Einhorn, T.A., et al., *The healing of segmental bone defects induced by demineralized bone matrix. A radiographic and biomechanical study*. J Bone Joint Surg Am, 1984. **66**(2): p. 274-9.

164. Yannas, I., *Natural Materials*, in *Biomaterials Science: An introduction to materials and methods*, B. Ratner, Hoffman, AS, Schoen, FJ, Lemons, JE, Editor. 1996, Academic Press: San Diego.
165. Cornell, C.N., *Osteoconductive materials and their role as substitutes for autogenous bone grafts*. *Orthop Clin North Am*, 1999. **30**(4): p. 591-8.
166. Kleinman, H.K., R.J. Klebe, and G.R. Martin, *Role of collagenous matrices in the adhesion and growth of cells*. *J Cell Biol*, 1981. **88**(3): p. 473-85.
167. Yunoki, S., et al., *Three-dimensional porous hydroxyapatite/collagen composite with rubber-like elasticity*. *J Biomater Sci Polym Ed*, 2007. **18**(4): p. 393-409.
168. Jancar, J., et al., *Mechanical response of porous scaffolds for cartilage engineering*. *Physiol Res*, 2007.
169. Niemeyer, P., et al., *Evaluation of mineralized collagen and alpha-tricalcium phosphate as scaffolds for tissue engineering of bone using human mesenchymal stem cells*. *Cells Tissues Organs*, 2004. **177**(2): p. 68-78.
170. Rodrigues, C.V., et al., *Characterization of a bovine collagen-hydroxyapatite composite scaffold for bone tissue engineering*. *Biomaterials*, 2003. **24**(27): p. 4987-97.
171. Bernhardt, A., et al., *Mineralised collagen-an artificial, extracellular bone matrix-improves osteogenic differentiation of bone marrow stromal cells*. *J Mater Sci Mater Med*, 2007.
172. Du, C., et al., *Three-dimensional nano-HAp/collagen matrix loading with osteogenic cells in organ culture*. *J Biomed Mater Res*, 1999. **44**(4): p. 407-15.
173. Urist, M.R., et al., *A bovine low molecular weight bone morphogenetic protein (BMP) fraction*. *Clin Orthop Relat Res*, 1982(162): p. 219-32.
174. Sammarco, V.J. and L. Chang, *Modern issues in bone graft substitutes and advances in bone tissue technology*. *Foot Ankle Clin*, 2002. **7**(1): p. 19-41.
175. Jiao, Y., Z. Liu, and C. Zhou, *Fabrication and characterization of PLLA-chitosan hybrid scaffolds with improved cell compatibility*. *J Biomed Mater Res A*, 2007. **80**(4): p. 820-5.
176. Whang, K., et al., *Engineering bone regeneration with bioabsorbable scaffolds with novel microarchitecture*. *Tissue Eng*, 1999. **5**(1): p. 35-51.
177. Liu, H.C., et al., *Preparation of PLLA membranes with different morphologies for culture of MG-63 Cells*. *Biomaterials*, 2004. **25**(18): p. 4047-56.
178. Lu, L., et al., *In vitro degradation of porous poly(L-lactic acid) foams*. *Biomaterials*, 2000. **21**(15): p. 1595-605.

179. Pihlajamaki, H., et al., *Long-term tissue response to bioabsorbable poly-l-lactide and metallic screws: An experimental study*. Bone, 2006.
180. Moran, J.M., D. Pazzano, and L.J. Bonassar, *Characterization of polylactic acid-polyglycolic acid composites for cartilage tissue engineering*. Tissue Eng, 2003. **9**(1): p. 63-70.
181. Daniels, A.U., M.K. Chang, and K.P. Andriano, *Mechanical properties of biodegradable polymers and composites proposed for internal fixation of bone*. J Appl Biomater, 1990. **1**(1): p. 57-78.
182. Chu, C.F., et al., *Enhanced growth of animal and human endothelial cells on biodegradable polymers*. Biochim Biophys Acta, 1999. **1472**(3): p. 479-85.
183. Lombello, C.B., et al., *Adhesion and morphology of fibroblastic cells cultured on different polymeric biomaterials*. J Mater Sci Mater Med, 2002. **13**(9): p. 867-74.
184. Nakagawa, M., et al., *Improvement of cell adhesion on poly(L-lactide) by atmospheric plasma treatment*. J Biomed Mater Res A, 2006. **77**(1): p. 112-8.
185. Yamaguchi, M., et al., *Surface modification of poly(L-lactic acid) affects initial cell attachment, cell morphology, and cell growth*. J Artif Organs, 2004. **7**(4): p. 187-93.
186. Cronin, E.M., et al., *Protein-coated poly(L-lactic acid) fibers provide a substrate for differentiation of human skeletal muscle cells*. J Biomed Mater Res A, 2004. **69**(3): p. 373-81.
187. Leenslag, J.W., et al., *Resorbable materials of poly(L-lactide). VII. In vivo and in vitro degradation*. Biomaterials, 1987. **8**(4): p. 311-4.
188. Kim, Y.J., et al., *A study of compatibility between cells and biopolymeric surfaces through quantitative measurements of adhesive forces*. J Biomater Sci Polym Ed, 2003. **14**(12): p. 1311-21.
189. Simon, C.G., Jr., et al., *Combinatorial screening of cell proliferation on poly(L-lactic acid)/poly(D,L-lactic acid) blends*. Biomaterials, 2005. **26**(34): p. 6906-15.
190. Wan, Y., et al., *Characterization of surface property of poly(lactide-co-glycolide) after oxygen plasma treatment*. Biomaterials, 2004. **25**(19): p. 4777-83.
191. Wan, Y., et al., *Adhesion and proliferation of OCT-1 osteoblast-like cells on micro- and nano-scale topography structured poly(L-lactide)*. Biomaterials, 2005. **26**(21): p. 4453-9.
192. Wan, Y., et al., *Cell adhesion on gaseous plasma modified poly-(L-lactide) surface under shear stress field*. Biomaterials, 2003. **24**(21): p. 3757-64.

193. Gao, J., L. Niklason, and R. Langer, *Surface hydrolysis of poly(glycolic acid) meshes increases the seeding density of vascular smooth muscle cells*. J Biomed Mater Res, 1998. **42**(3): p. 417-24.
194. Barry, J., M. Silva, K. Shakesheff, S. Howdle, M. Alexander, *Using plasma deposits to promote cell population of the porous interior of three-dimensional poly(D, L-Lactic Acid) Tissue-Engineering scaffolds*. Advanced Functional Materials, 2005. **15**: p. 1134-1140.
195. Lee, J.H., et al., *Cell behaviour on polymer surfaces with different functional groups*. Biomaterials, 1994. **15**(9): p. 705-11.
196. Lee, J.H., et al., *Interaction of Different Types of Cells on Polymer Surfaces with Wettability Gradient*. J Colloid Interface Sci, 1998. **205**(2): p. 323-330.
197. Ma, Z., et al., *Chondrocyte behaviors on poly-L-lactic acid (PLLA) membranes containing hydroxyl, amide or carboxyl groups*. Biomaterials, 2003. **24**(21): p. 3725-30.
198. Lee, J.H., J.W. Park, and H.B. Lee, *Cell adhesion and growth on polymer surfaces with hydroxyl groups prepared by water vapour plasma treatment*. Biomaterials, 1991. **12**(5): p. 443-8.
199. Sikavitsas, V.I., et al., *Mineralized matrix deposition by marrow stromal osteoblasts in 3D perfusion culture increases with increasing fluid shear forces*. Proc Natl Acad Sci U S A, 2003. **100**(25): p. 14683-8.
200. Schultz, S.S. and P.A. Lucas, *Human stem cells isolated from adult skeletal muscle differentiate into neural phenotypes*. J Neurosci Methods, 2006. **152**(1-2): p. 144-55.
201. Knippenberg, M., et al., *Adipose tissue-derived mesenchymal stem cells acquire bone cell-like responsiveness to fluid shear stress on osteogenic stimulation*. Tissue Eng, 2005. **11**(11-12): p. 1780-8.
202. Leong, K.F., C.M. Cheah, and C.K. Chua, *Solid freeform fabrication of three-dimensional scaffolds for engineering replacement tissues and organs*. Biomaterials, 2003. **24**(13): p. 2363-78.
203. Grinnell, F., *Cellular adhesiveness and extracellular substrata*. Int Rev Cytol, 1978. **53**: p. 65-144.
204. Mikos, A.G., et al., *Wetting of poly(L-lactic acid) and poly(DL-lactic-co-glycolic acid) foams for tissue culture*. Biomaterials, 1994. **15**(1): p. 55-8.
205. van Wachem, P.B., et al., *Interaction of cultured human endothelial cells with polymeric surfaces of different wettabilities*. Biomaterials, 1985. **6**(6): p. 403-8.

206. Alves, C.M., et al., *Modulating bone cells response onto starch-based biomaterials by surface plasma treatment and protein adsorption*. *Biomaterials*, 2007. **28**(2): p. 307-15.
207. Wilson, C.J., et al., *Mediation of biomaterial-cell interactions by adsorbed proteins: a review*. *Tissue Eng*, 2005. **11**(1-2): p. 1-18.
208. Dhawan, S., R.L. Fields, and F.A. Robey, *A novel peptide from amyloid P component supports cell attachment*. *Biochem Biophys Res Commun*, 1990. **171**(3): p. 1284-90.
209. Underwood, P.A. and F.A. Bennett, *A comparison of the biological activities of the cell-adhesive proteins vitronectin and fibronectin*. *J Cell Sci*, 1989. **93** (Pt 4): p. 641-9.
210. Lee, R.H., et al., *Characterization and expression analysis of mesenchymal stem cells from human bone marrow and adipose tissue*. *Cell Physiol Biochem*, 2004. **14**(4-6): p. 311-24.
211. Romanov, Y.A., et al., *Mesenchymal stem cells from human bone marrow and adipose tissue: isolation, characterization, and differentiation potentialities*. *Bull Exp Biol Med*, 2005. **140**(1): p. 138-43.
212. Gronthos, S., et al., *Surface protein characterization of human adipose tissue-derived stromal cells*. *J Cell Physiol*, 2001. **189**(1): p. 54-63.
213. Katz, A.J., et al., *Cell surface and transcriptional characterization of human adipose-derived adherent stromal (hADAS) cells*. *Stem Cells*, 2005. **23**(3): p. 412-23.
214. Shur, I., et al., *Adhesion molecule expression by osteogenic cells cultured on various biodegradable scaffolds*. *J Biomed Mater Res A*, 2005. **75**(4): p. 870-6.
215. Richardson, S.M., et al., *The differentiation of bone marrow mesenchymal stem cells into chondrocyte-like cells on poly-L-lactic acid (PLLA) scaffolds*. *Biomaterials*, 2006. **27**(22): p. 4069-78.
216. Wente, V., *Superfine thermoplastic fibers*. *Industrial and Engineering Chemistry*, 1956. **48**(8): p. 1342-1346.
217. Zhao, R., Wadsworth LC, *Attenuating PP/PET bicomponent melt blown microfibers*. *Polymer Engineering and Science*, 2003. **43**(2): p. 463-469.
218. Xu, B., Pourdeyhimi, B., Sobus, J, *Fiber Cross-Sectional Shape Analysis Using Image Processing Techniques*. *Textile Research Journal*, 1993. **63**(12): p. 717-730.
219. Pourdeyhimi, B., Xu, B. *Pore Size and Fiber Orientation in Nonwoven Fabrics*. in *The Fiber Society*. 1993. Raleigh, NC.
220. Shimko, D.A. and E.A. Nauman, *Development and characterization of a porous poly(methyl methacrylate) scaffold with controllable modulus and permeability*. *J Biomed Mater Res B Appl Biomater*, 2006.

221. Taqvi, S. and K. Roy, *Influence of scaffold physical properties and stromal cell coculture on hematopoietic differentiation of mouse embryonic stem cells*. *Biomaterials*, 2006. **27**(36): p. 6024-31.
222. Yang, F., et al., *Characterization of neural stem cells on electrospun poly(L-lactic acid) nanofibrous scaffold*. *J Biomater Sci Polym Ed*, 2004. **15**(12): p. 1483-97.
223. Toh, Y.C., Ng S, Khong Y.M., Zhang X, Zhu Y, Lin P.C., Te C.M., Sun W, Yu H, *Cellular responses to a nanofibrous environment*. *Nanotoday*, 2006. **1**(3): p. 34-43.